

UCSF

UC San Francisco Electronic Theses and Dissertations

Title

An Evaluation of Facial Asymmetry Using Three-Dimensional Cone-Beam Computed Tomography

Permalink

<https://escholarship.org/uc/item/8ds5n9x7>

Author

Laurent, Caroline

Publication Date

2009

Peer reviewed|Thesis/dissertation

**An Evaluation of Facial Asymmetry Using Three-Dimensional Cone-Beam Computed
Tomography**

by

Caroline A. Laurent, D.M.D.

THESIS

Submitted in partial satisfaction of the requirements for the degree of

MASTER OF SCIENCE

in

ORAL AND CRANIOFACIAL SCIENCES

in the

GRADUATE DIVISION

of the

UNIVERSITY OF CALIFORNIA, SAN FRANCISCO

DEDICATION

I would like to dedicate this thesis to my parents who have supported me through my many years of school and have truly been inspirations for their children. Thank you for living by example and reminding me that anything really is possible.

ACKNOWLEDGEMENTS

I would like to acknowledge the help of my research committee members, Dr. Karin Vargervik, Dr. John Huang, Dr. Janice Lee, and Dr. Sneha Oberoi for their invaluable guidance and input, both logistical and conceptual throughout this process. Drs. Vargervik and Oberoi guided my knowledge and understanding of asymmetry, especially related to orthodontic treatment. Dr. Lee helped me stay focused on the real world clinical application of this work, and Dr. Huang's knowledge of CBCT was crucial in understanding the validity and limitations of this process. Thank you all for your varied contributions to the ultimate project.

Additionally, I would like to acknowledge Dr. Art Miller and my four classmates for listening patiently and supportively over the past three years as I designed and modified this project substantially. Thank you for your input and friendship as this project developed.

An Evaluation of Facial Asymmetry Using Three-Dimensional Cone-Beam Computed Tomography

Caroline A. Laurent, DMD

Aims: In the fields of orthodontics and dentofacial orthopedics, oral and maxillofacial surgery, and craniofacial anomalies, a method to precisely identify, quantify, and diagnose facial asymmetries would be invaluable in the treatment and outcome of individuals with marked asymmetries. To date no studies have been published on asymmetry in living subjects using CBCT as an assessment tool. The aims of this study were to identify quantifiable differences between subjects with and without clinical asymmetry, to develop a practical, reproducible, user-friendly method of analyzing patients' symmetry in three dimensions using cone beam computed tomography and Dolphin 3D imaging software, and to quantify the amount of asymmetry in clinically symmetric patients.

Materials and Methods: The cone beam computed tomography three dimensional scans of subjects presenting to the University of California San Francisco graduate orthodontic clinic were evaluated using traditional and novel points to study mandibular asymmetry. Thirty three individuals with no clinical asymmetry or midline deviation were selected as the control group and nineteen individuals with a chin point deviation were included in the asymmetry group. The scans were oriented in a novel, standardized method, then sixteen landmarks and twelve linear and angular measurements were studied. The average three dimensional difference between the right and left sides was calculated and graphically represented as an asymmetry index for the control group. Individual asymmetric subject's data was compared to this graphical norm to determine the specific location of asymmetry.

Results: Error associated with the orientation method ranged from 0.83-2.09mm. In the control group, asymmetry ranged from 0.74mm for nasal height to 3.49mm for gonion. In the asymmetry group, asymmetry ranged from 0.71mm for ANS to 5.97mm for mandibular foramen.

Conclusion: Substantial error, both in the orientation method and landmark identification, is associated with this method of three dimensional analysis. Statistical differences were found between mandibular points in two study groups. Although the analysis needs refinement, it can be used to identify the location of asymmetry in subjects with chin deviation and will be useful in the proper diagnosis, understanding, and treatment of individuals with these asymmetries.

TABLE OF CONTENTS

DEDICATION	iii
ACKNOWLEDGEMENTS	iv
ABSTRACT	v
TABLE OF CONTENTS	vi
LIST OF TABLES	viii
LIST OF FIGURES	ix
INTRODUCTION	1
Types of Asymmetry	2
Methods of Evaluation	3
Evaluation of Asymmetry in Clinically Symmetric Individuals	4
Evaluation of Asymmetry in Clinically Asymmetric Individuals	6
Errors in Cephalometric Evaluation of Asymmetry	7
Cone Beam Computed Tomography	9
Evaluation of Asymmetry with Three-Dimensional Radiography	11
Rationale for Continued Investigation of Asymmetry	13
Hypothesis	15
Purpose	15
MATERIALS AND METHODS	16
Subjects	16
CBCT/Landmark Identification Software	17
Testing the Orientation Method	17
Landmark Identification	20
Evaluation of Landmarks	22
RESULTS	24
Reliability of Orientation Method	24
Reproducibility of Study Landmarks and Measurements	29
Asymmetry Index Values	35
DISCUSSION	39
Reproducibility of Head Orientation	39

Reproducibility of Landmark Identification	40
Asymmetry in Symmetric Subjects	41
Asymmetry in Asymmetric Subjects	42
Clinical Application of Findings	43
Examples	45
CONCLUSION	49
REFERENCES	52
PUBLISHING AGREEMENT	57

LIST OF TABLES

Table 1 – Definition of landmarks identified using Dolphin Imaging Software	21
Table 2 - Definition of linear and angular measurements taken using Dolphin Imaging Software	22
Table 3 – The mean difference and standard deviation in millimeters between repeated time points for ten landmarks with high inter-rater reliability on five subjects	28
Table 4 – The mean three-dimensional error in millimeters of ten highly reproducible landmarks on five subjects and the amount of error calculated from landmark identification without error for head orientation	29
Table 5 – Mean difference and standard deviation of repeated landmark measurements, in millimeters	34
Table 6 – Mean difference and standard deviation for linear and angular measurements, in millimeters or degrees	35
Table 7 – Mean and standard deviation of the Asymmetry Index values for both clinically symmetric and asymmetric subjects	36

LIST OF FIGURES

Figure 1 – A diagrammatic chart to classify the degree of deformity in facial asymmetry patients	13
Figure 2 – Graphic representation of the linear regression analysis of repeated measures of the X axis from five repeated scans, used to evaluate the orientation method	25
Figure 3- Graphic representation of the Bland-Altman test for the X axis from five repeated scans, used to evaluate the orientation method	25
Figure 4 - Graphic representation of the linear regression analysis of repeated measures of the Y axis from five repeated scans, used to evaluate the orientation method	26
Figure 5 – Graphic representation of the Bland-Altman test for the Y axis from five repeated scans, used to evaluate the orientation method	26
Figure 6 – Graphic representation of the linear regression analysis of repeated measures of the Z axis from five repeated scans, used to evaluate the orientation method	27
Figure 7 - Graphic representation of the Bland-Altman test for the Z axis from five repeated scans, used to evaluate the orientation method	27
Figure 8 – Graphic representation of the linear regression analysis of repeated measures of the X axis, used to evaluate the landmark reproducibility from ten repeated scans	30
Figure 9 – Graphic representation of the Bland-Altman test for the X axis, used to evaluated landmark reproducibility from ten repeated scans	30
Figure 10 – Graphic representation of the linear regression analysis of repeated measures of the Y axis, used to evaluate the landmark reproducibility from ten repeated scans	31
Figure 11- Graphic representation of the Bland-Altman test for the Y axis, used to evaluated landmark reproducibility from ten repeated scans	31
Figure 12 – Graphic representation of the linear regression analysis of repeated measures of the Z axis, used to evaluate the landmark reproducibility from ten repeated scans	32

Figure 13- Graphic representation of the Bland-Altman test for the Z axis, used to evaluated landmark reproducibility from ten repeated scans	32
Figure 14 – Graphic representation of the linear regression analysis of repeated measures of the linear and angular measurements, used to evaluate the landmark reproducibility from ten repeated scans	33
Figure 15 - Graphic representation of the Bland-Altman test for the linear and angular measurements, used to evaluated landmark reproducibility from ten repeated scans	33
Figure 16 – Asymmetry Index for subjects without clinical asymmetry, listed by anatomical region	38
Figure 17 – Subject CLMP39	45
Figure 18 – The individual overlay of subject CLMP39	46
Figure 19 – Subject CLMP18	47
Figure 20 – The individual overlay of subject CLMP18	48

An Evaluation of Facial Asymmetry Using Three-Dimensional Cone-Beam Computed Tomography

INTRODUCTION

Humans exhibit, in general, bilateral symmetry. However, true bilateral symmetry is only a theoretical concept, applicable to large populations but seldom, if ever, to the individual.¹ Nearly every person exhibits some degree of asymmetry, as shown by various studies using composite pictures reflecting two right or two left sides of a face^{1,2} or critical evaluation of clinically symmetric individuals.^{3,4} Historically, even great works of art, such as the Venus de Milo, show some degree of asymmetry and yet are still generally considered beautiful.¹ Asymmetry develops in response to the environmental factors over-riding the genetic code which defines the bilateral symmetry of an organism. Therefore, while perfect symmetry of the face and head may be considered “ideal”, in most cases it is not an achievable, or even desirable, goal.²

Some individuals, however, develop marked asymmetries that require orthodontic and potentially surgical correction to improve their dental function and facial esthetics. Analysis of these individuals has been difficult due to the complexity of the asymmetry and the limitations of existing two-dimensional imaging modalities. The asymmetry is often manifested in all three planes of space, yet the overlapping structures observed on two-dimensional radiographs can significantly compromise a clinician’s ability to properly diagnose and treat the origin of the problem. Additionally, if researchers were

able to more thoroughly study patient growth patterns, decisions could be made regarding treatment timing to maximize efficacy. Three-dimensional cone-beam computed tomography (CBCT) was introduced to the dental profession in 1999 and in the United States in 2001. This technology can theoretically overcome many of the limitations of two-dimensional radiography and aid clinicians in diagnosing and studying individuals with asymmetries.

Types of Asymmetry

Lundström¹ describes how one may evaluate craniofacial asymmetries as it relates to the field of orthodontics. The asymmetry may be qualitative such as missing teeth or clefts of the lip and palate, quantitative such as size of teeth and antero-posterior, lateral, or vertical position of teeth in the dental arches, or caused by rotations in the horizontal, lateral, or frontal planes. The quantitative variants are expressed in a range of asymmetries from clinically “normal” to the most severe types of hemifacial microsomia or hypertrophy.

Cheney⁵ describes four types of asymmetries: unilateral antero-posterior displacements, vertical displacements, lateral displacements, and rotary displacements. Each of these clinical situations results from an unequal growth of the dentofacial components. However, some situations may be exacerbated by a compensatory muscular adaptation, such as a lateral functional dental shift due to a narrow maxilla or anterior dental relationship causing an anterior shift of the mandible. Still other acquired

asymmetries are only dental in nature. These asymmetries may result from finger sucking habits, asymmetric chewing habits, loss of contact points through dental caries, extraction of primary or permanent teeth, or trauma.¹ Understanding the exact size, shape, and position of the underlying asymmetrical parts is necessary to properly diagnose and treat individuals with these asymmetries.

Methods of Evaluation

Traditionally, standard postero-anterior (PA) cephalograms are used to evaluate vertical and horizontal asymmetry. Great variation exists between the methods of analyses of these radiographs. Some investigators choose to use triangulation of points, comparing the areas of the bilateral surfaces.^{6,7} Other investigators use the difference in distance between bilateral points in reference to a center line,^{8,9} while others prefer a best fit line to midline structures.¹⁰ Though many investigators have proposed methods of analyzing asymmetry,¹¹ none have gained universal acceptance, presumably because of the many limitations of two-dimensional radiography in evaluating of a three-dimensional problem.

In order to fully appreciate the three-dimensionality of asymmetry using traditional two-dimensional films, one must combine several two-dimensional radiographs from different angles into a three dimensional format.⁵ This is a cumbersome and difficult undertaking, requiring some combination of lateral, lateral open-mouth, postero-anterior cephalograms, and submental vertex radiographs with

superimposition of dental casts and facial photographs.¹²⁻¹⁴ All of these analyses use equations and novel points to evaluate the radiographic data. While the investigators claim their methods are practical and can be used in the clinical setting, most protocols seem overwhelming for the average practitioner to use with any regularity.

Evaluation of Asymmetry in Clinically Symmetric Individuals

Despite the numerous limitations of analyzing asymmetry using two-dimensional radiographs, for many years that was the only option for clinicians and researchers. Many studies have been conducted to investigate the degree of asymmetry in clinically symmetric individuals. After studying the PA cephalograms of 63 clinically symmetric subjects using a triangulation system of analysis, Vig and Hewitt⁶ found that the zygomatic and nasal areas of the face were significantly different in this sample, while the maxillary and mandibular regions were statistically indistinguishable. In this study, the left side of the face was found to be larger than the right. Lundstrom measured 29 skulls and also saw a tendency towards an enlarged left side of the skull, also reported by other investigators.¹ Conversely, Shah and Joshi⁷ examined 43 clinically symmetric individuals using PA cephalograms and a technique similar to Vig and Hewitt. These investigators noted that the total facial structure, overall maxillary area, and, specifically, the lateral maxillary area were larger on the right.

Letzer¹⁵ used a different technique involving a simple set of angles on PA cephalometric x-rays to evaluate asymmetry in 50 individuals with natural “excellent”

occlusion and 50 with a malocclusion, not specifically asymmetric. He found that 20% of the excellent occlusion individuals exhibited asymmetry in the anterior cranial base and mandible. In the malocclusion group, 40% had asymmetry of the cranial base and 77% showed asymmetry of the mandible.

Good *et al.*¹⁶ examined 66 individuals who sought orthodontic treatment and observed that twice as many individuals with a class III malocclusion exhibited asymmetry of the lower face when compared to class I or II, who were similar. Additionally, they found that individuals with an increased lower anterior face height had a higher incidence of mandibular asymmetry compared to those with a normal or reduced lower anterior face height.

In a study by Haraguchi *et al.*, facial photographs were taken on a sample of 1800 untreated Japanese orthodontic subjects, varying in age and malocclusion.¹⁷ Though the measurements were simple, and only the width of the face and chin deviation were examined, they discovered that approximately 80% demonstrated facial asymmetry and 60% demonstrated a measureable chin deviation regardless of age, sex, growth stage, or skeletal pattern. Interestingly, they noted that nearly 80% of the subjects demonstrated a wider right hemiface and the same percentage had a left-sided chin deviation.

Evaluation of Asymmetry in Clinically Asymmetric Individuals

Individuals with a class II subdivision malocclusion present a unique challenge to clinicians in determining whether the observed asymmetry is skeletal or dental. Azevedo *et al.*¹⁸ studied 23 subjects with a class II subdivision malocclusion and 30 control subjects. They evaluated a submental vertex and PA cephalogram of each individuals using linear measurements of bilateral points to a central coordinate system. Their results indicated that the class II malocclusion was predominantly dentoalveolar in nature, with a small amount of mandibular asymmetry. It should be noted that the “normal occlusion” group exhibited between 1.33-mm and 4.25-mm bilateral asymmetry on the skeletal measurements, with anterior nasal spine as the most symmetric and antegonial notch as the least symmetric. This confirms earlier work done by this group using submental vertex, PA cephalometric, and right and left lateral oblique radiographs.¹⁹

Individuals with class III malocclusion also exhibit mandibular asymmetry. Haraguchi *et al.*²⁰ examined 220 Japanese adults with a class III malocclusion using a PA cephalogram. They measured midline points to a midline reference line. Any variation greater than 2-mm was considered asymmetric. They discovered 80% of the subjects in this sample exhibited mandibular skeletal asymmetry, while only 56% showed soft tissue asymmetry.

Individuals with severe skeletal deformities present unique challenges for investigation and analysis. Individuals with complete unilateral cleft lip and palate

(UCLP) have an obvious maxillary asymmetry. Laspos *et al.*²¹ studied 40 UCLP subjects to evaluate the degree of maxillary and mandibular asymmetry in the vertical and transverse planes, as seen in postero-anterior cephalometric radiographs. This study found that UCLP subjects were more asymmetric in the maxillary vertical and transverse planes when compared to age matched non-cleft subjects. The UCLP individuals also had greater mandibular asymmetry, which paralleled the asymmetry of the maxilla.

Errors in Cephalometric Evaluation of Asymmetry

Landmark identification error is a topic that is important to any study of cephalometric radiographs. In a classic paper from 1971, Baumrind *et al.*²² studied the “nature and magnitude of the difference in precision with which we identify the different landmarks used in standard cephalometric analyses.” His three conclusions are relevant in light of analysis of asymmetry and in the advent of three dimensional analyses: (1) errors in landmark identification are too great to ignore; (2) the magnitude of error varies greatly between landmarks; (3) the distribution of errors is specific to that particular landmark.

Studies have been conducted to look at error in antero-posterior headfilms as well. Savara *et al.*²³ studied the reproducibility of mandibular linear and angular measurements on seven year old children. They traced a lateral, lateral open mouth, and frontal cephalogram for each child and converted the findings into linear measurements. They

found that the variation of measurements, both within and between examiners, was approximately 15-37% of the value of the measurement.²³

Major *et al.*²⁴ evaluated 33 dry skulls and 25 clinically symmetric individuals using 52 landmarks. They found intra-examiner error to be 0.28-2.23mm while inter-examiner reliability was shown to be between 0.31-4.79mm.²⁴ They found, similar to Baumrind, that points have specific patterns of error. This is important because points with a large horizontal error but a small vertical error could be used for measurements in the vertical dimension, but should be used cautiously for interpretations relative to the horizontal plane. Additionally, some landmarks had small intra-examiner error, but large inter-examiner error. These landmarks may be useful in research studies where one operator makes repeated measures, but would have limited clinical application. They suggest that “landmarks with identification errors greater than 1.5-mm should probably be avoided and landmarks with identification error greater than 2.5-mm are inappropriate.”²⁴ In a subsequent paper, Major *et al.*²⁵ described the effect of head rotation on landmark identification. Some landmarks were significantly affected by rotation of the skull, but many were within their 1.5-mm of acceptability. These measurements, however, were done on skulls, which was shown to be more accurate than on live subjects.²⁴

El Mangoury *et al.*²⁶ evaluated 40 PA cephalograms for landmark reliability on the same cephalogram. They found radial errors ranging from 0.93 ± 0.07 mm for point B to 2.08 ± 1.93 mm for the lower first molar. The conclusions of this paper were similar to

those stated by Baumrind regarding lateral cephalometric error. They found skeletal landmarks to be more reliable than dental landmarks and “most cephalometric landmarks have their own peculiar noncircular envelope of error. In other words, most landmarks are more difficult to locate in one direction than another.”²⁶

Another issue affecting the reliability of cephalometric analyses is the effect of film-object distance. Ghafari *et al.*²⁷ studied seventeen skulls with varying film-object distances and varying angulation from the Frankfort horizontal plane. They found no difference in measurements at the different film-object distances and suggest a film-object distance of 13-cm as a standard. Additionally, there were no differences in the horizontal measurements with a change in head inclination of up to ten degrees; however, vertical measurements were affected. They did not evaluate rotation around planes other than Frankfort horizontal to determine the influence of that distortion on asymmetry analysis.

Cone Beam Computed Tomography

Medical spiral computed tomography technology (medCT) has been available since 1972 and used to evaluate individuals with craniofacial deformities.²⁸⁻³¹ The imaging provides a clear, reconstructed three-dimensional representation of the craniofacial region. Some of the benefits include a lack of magnification that is seen in traditional cephalometrics and a lack of superimposition of the structures. However, this technology is not without limitations, including the high radiation dose, window setting

scan noise, artifacts, spatial uniformity, resolution, relative difficulty of access and high cost.³²

Cone beam computed tomography (CBCT) was introduced to the United States market in 2001 as an alternative to traditional medCT with significant advantages of lower radiation dose and cost. The variations among machines are substantial. One study found the effective radiation dose to be 4-42 times greater than that of a panoramic radiograph, though substantially lower than a medCT.³³ A thorough comparative review of CBCT versus medCT concluded that while medCT has technical advantages in critical fields such as pulmonology and cardiology, CBCT is an adequate, lower dose method of obtaining reliable three-dimensional images of the craniofacial region.³⁴

Recent studies have examined the reliability of craniofacial landmark identification and analysis based on medCT and CBCT scans. Studies have found that landmark identification and linear measurements were consistent between lateral cephalograms or dry skulls and reconstructed medCT scans.^{32,35} Kragstov *et al.*³⁶ found that the variation was higher overall when the same points were studied on cephalograms versus medCT. Points related to a frontal radiograph showed even higher variation, ranging from approximately 1-3 mm. Stratemann *et al.*³⁷ showed that the difference between measurements on dry skulls and the CB Mercuray was 0.00 ± 0.22 mm. From these studies, one can be confident that CBCT can be used accurately as a three-dimensional imaging tool for studying the craniofacial region.

Evaluation of Asymmetry with Three-dimensional Radiography

The limitations of two-dimensional radiography have been discussed and the introduction and availability of medCT and CBCT has interested many groups studying craniofacial asymmetry. Maki *et al.*³⁰ examined 32 subjects with asymmetrical mandibles using medCT. While the primary focus of the paper was analyzing cortical bone mineral density, their analysis of the asymmetric mandibles also included three-dimensional descriptive measurements of the asymmetric mandibles. Their primary measurements for mandibular length used a novel system based on identifying the three-dimensional center of the condyle and mandibular symphysis. The investigators found the differences vary from 3-21 mm between right and left sides.

Kwon *et al.*²⁹ evaluated the morphological characteristics of the craniofacial region to determine if clinical mandibular asymmetry in their study sample was a result of primary mandibular deformity or if it was influenced by cranial base deformity. They examined 24 individuals with clinical chin point deviation and 18 symmetric subjects using medCT reformatted images. They discovered that the degree of cranial base asymmetry was not significantly different between the two groups and concluded that cranial measurement variables were not the dominant factors that determined the degree of facial asymmetry. A second group found no difference between the cranial base in subjects with and without chin point deviations, as evaluated by medCT.³⁸

Three-dimensional computed tomography was also used by Katsumata *et al.*³⁹ to develop an asymmetry index that calculated the variation of each point in millimeters. Based on 16 control subjects, they developed a diagrammatic chart to evaluate asymmetry. Their reference planes were constructed through the following landmarks:

- x-axis (midsagittal) reference plane: through points sella turcica (S), nasion (N), and the odontoid process of the epistropheus (Dent)
- y-axis (coronal) reference plane: perpendicular to the x-axis and included points S & N
- z-axis (axial) reference plane: perpendicular through the x-axis and included Dent point.

The landmarks were identified and the length of the 3-D vector to each point from the intersection of the three reference planes (dx, dy, and dz) was calculated. The asymmetry index of each bilateral point was the difference in the length of the 3-D vectors on the right versus left sides, calculated with the following equation: $\sqrt{(Rdx-Ldx)^2+(Rdy-Ldy)^2+(Rdz-Ldz)^2}$. They found reproducibility to be 4.6% for dx, 3.2% for dy, and 2.2% for dz. They also found the asymmetry indexes to be 0.8-4.6 mm with a standard deviation of 0.7-1.7mm. Graphic representation of their data is shown in Figure 1. Gonion was the most asymmetric point and anterior nasal spine was the least. From this work, they proposed a novel method of analyzing and diagnosing individuals with clinical asymmetries. In their discussion, they note that taking spiral CTs for the purpose of diagnosis or research is no longer allowed due to unacceptable radiation exposure.

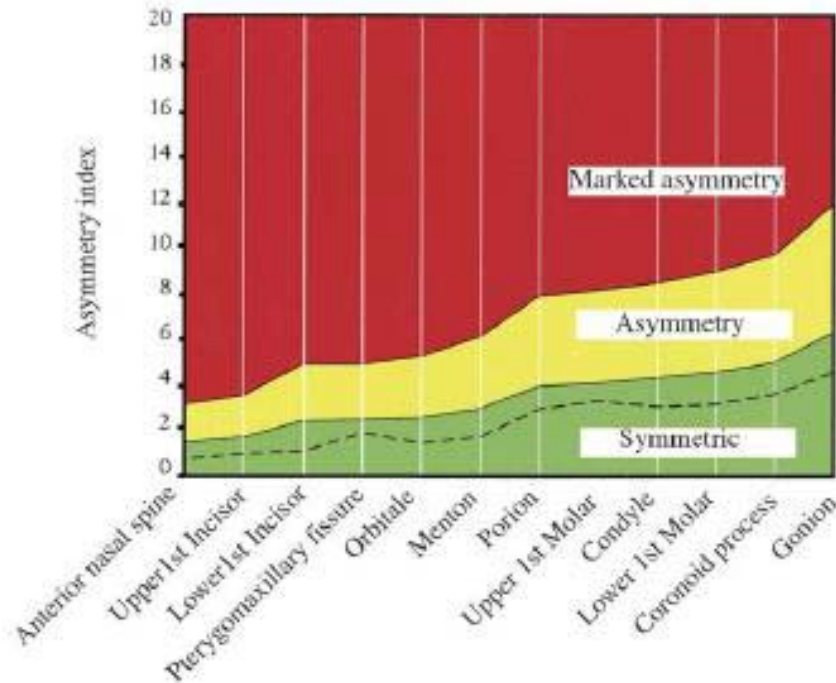


Figure 1. A diagrammatic chart to classify the degree of deformity in facial asymmetry patients. When the asymmetry index of a patient's anatomical point was in the green, yellow, and red areas, the point was diagnosed as "Symmetric," "Asymmetry," and "Marked Asymmetry," respectively. A line between the green and yellow areas indicates the mean asymmetry indexes plus the standard deviation of each anatomical point. The line between the yellow and the red areas indicates twice the baseline value. The dotted line indicates the mean asymmetry indexes. Copied from Katsumata et al. 2005.³⁹

Rationale for Continued Investigation of Asymmetry

Clearly, with all the areas of possible asymmetry, asymmetries are not easy to define or quantify. In the fields of orthodontics and dentofacial orthopedics, oral and maxillofacial surgery, and craniofacial anomalies, a method to precisely identify,

quantify, and diagnose facial asymmetries would be invaluable in the treatment and outcome of individuals with marked asymmetries. Mulick⁹ in 1965 stated:

It is clear that a method must be devised which will accurately define and assess the areas of asymmetry in the craniofacial region, thereby providing limits and ranges useful for future comparison. This method could be applied in the study of special asymmetry, such as cleft lip and cleft palate, condylar and facial dysplasias, and many of the hereditary syndromes involving the face and cranium. Such a method could also be used in the pretreatment and post-treatment assessment of orthodontic, surgical, and prosthetic patients with one of these types of asymmetry. Investigations using this technique could provide valuable information regarding the cause of certain types of asymmetry.

Based on the technology and resources available at the time, Mulick's proposed method of studying and quantifying this asymmetry involved translation of AP and lateral cephalograms into three-dimensional Cartesian co-ordinate systems with complex measurements and mathematics. While his goals are still extremely valid, now with the advent of three-dimensional cone beam computed tomography a new tool exists to more easily and accurately reach these goals. To date no studies have been published on asymmetry in living subjects using CBCT as an assessment tool.

Hypothesis

Quantifiable differences can be identified between individuals with and without clinical asymmetry.

Purpose

To identify quantifiable differences between individuals with and without clinical asymmetry.

To develop a practical, reproducible, user-friendly method of analyzing asymmetry in three dimensions using cone beam computed tomography and Dolphin 3D imaging software.

To quantify the amount of asymmetry in clinically symmetric individuals.

MATERIALS AND METHODS

Subjects

Subjects were selected from individuals who presented to the University of California, San Francisco (UCSF) Graduate Orthodontic Clinic during the 2006-2008 academic years and received a CBCT as their initial diagnostic imaging record. Subjects with prior orthodontic treatment, craniofacial syndromes, multiple missing teeth, or anticipated growth remaining were excluded. No subjects were excluded due to malocclusion, (e.g. open bite, class II or III, excessive overjet, or crowding). After identification of the potential subjects, the investigator examined their facial photographs to confirm the presence or absence of facial/jaw symmetry as noted in the clinical record.

Subjects included in the control group (n=33) were individuals judged by an orthodontic resident to have no facial asymmetry upon clinical examination, and a dental and facial midline discrepancy of 1 mm or less. Subjects included in the clinically asymmetric group (n=19) were judged to have a chin point deviation indicative of mandibular asymmetry.

From the total 52 Dicom scans, ten scans were randomly selected for test for intra-operator error. The 62 data sets (52 subjects plus ten repeats) were imported into the Dolphin Imaging Software Program version 10.1 (Chatsworth, CA) in order to identify anatomic landmarks using the three-dimensional data. Each patient was assigned a random identifier to prevent any bias and to preserve privacy.

CBCT/Landmark Identification Software

A Hitachi CB MercuRay (Hitachi Medico Technology, Tokyo, Japan) charge-coupled sensor device was used for all patient scans and operated by the same certified radiologic technologist. With the patient sitting upright, a rotating source gantry captures an image of the subject's head, a process similar in nature to panoramic radiography. A 10-second scan acquires 288 primary images in a 12" diameter spherical volume with 0.376 mm³ voxel and 12 bit ($2^{12} = 4096$ shades of gray) resolution. In order to capture anatomy critical for orthodontic diagnosis and treatment planning, the 12-inch field of view was used. The x-ray source was generated with a wattage of 120-KvP and a current of 15-mA for each scan.

Testing the Orientation Method

Scans must be reproducibly oriented, since the measurements acquired are in millimeters from the reference planes. If the orientation is not reproducible, the error of landmark identification will be inaccurate and inflated. To test the orientation method of the CBCT three-dimensional reconstruction of the patient scans, five CBCT scans were randomly selected from the list of current DICOM files on the UCSF CBCT server. These five scans were each given two random identifiers and loaded into the Dolphin Imaging Software. All scans were oriented according to the following criteria.

- The sagittal orientation plane passed through the inferior aspect of the zygomatico-frontal suture and parallel to the sella-nasion line.

- The axial orientation plane passed through nasion and opisthion.
- The coronal orientation plane bisected clivus, where the inferior border is a straight line.

The Dolphin imaging software allows manipulation of the image to place the landmark point on any of the four available views: sagittal, transverse, vertical, and volumetric. The software updates the location of the point in all four views simultaneously to ensure that the placement of the landmark is satisfactory. The views display the three planes in a 0.3mm thick slice.

After the scans were saved in this orientation position, ten landmarks were identified. In a previous study by Schlicher,⁴¹ landmarks were identified on three-dimensional CBCT reconstructions of patient scans using Dolphin 3-D Imaging software, but with a standard skull orientation. The points with the greatest inter-examiner reliability were used to test the orientation method in this current study. These included sella, basion, nasion, right maxillary incisor tip, left maxillary incisor tip, anterior nasal spine, menton, gnathion, left mandibular incisor tip, and left mandibular incisor root apex.

The first five scans, one of each subject, were oriented and the listed points were identified. The procedure was repeated again three days later. The output from the Dolphin Imaging Software is generated as three-dimensional millimeter measurements from the 0,0,0 point, which was the intersection of the three orientation planes listed

above. These output values were compared for repeatability of the orientation method using the Bland-Altman test for all three dimensions (x-, y-, and z- planes) and the results are graphed with the confidence intervals. A correlation coefficient was also found for all three dimensions.

The mean difference between the two time points was averaged using the absolute value of the points to eliminate distortion based on right or left side error. A three-dimensional mean difference was calculated with the equation:

$$3D \text{ error} = \sqrt{(x_{\text{mean error}}^2 + y_{\text{mean error}}^2 + z_{\text{mean error}}^2)}$$

This was defined as the overall three-dimensional error in reproducing a given landmark between two time points.

The data from Schlicher's thesis⁴¹ were used to calculate the mean three dimensional error of each point using the equation above. This inter-rater error was defined as error of identification of the point, since all participants used CBCT scans with identical and fixed head orientation. The equation for error of the identification method was calculated as:

Overall error (data from this study, which included head orientation and point identification) – Point identification error (data from Schlicher's thesis, with only point identification and identical head orientation) = Error of identification method

Landmark Identification

The test scans were loaded into the Dolphin Imaging Software and then oriented according to the previously listed guide planes. The sixteen landmarks and ten linear measurements listed and defined in Tables 1 and 2 were identified on all test scans.

Many of these landmarks are defined as most extreme position in a given plane, for example, most superior, demonstrating the need for a reproducible orientation of the head. The definitions were described in this way because in cases of severe asymmetry, especially in type III hemifacial microsomia, certain landmarks are abnormal or missing, so traditional definitions would be insufficient.

These landmarks were chosen for their relevance to the study of craniofacial and, specifically, mandibular asymmetry. Many classical cephalometric landmarks, for example sella and nasion, are not included in this study because of the emphasis on asymmetry. Other landmarks, such as maxillary tuberosities, zygomatic processes, and mental foramen, are novel points included in this study to determine if their positions on the three-dimensional scan will aid in our understanding of the asymmetric skull. There is no universally accepted set of landmarks or measurements in the three-dimensional analysis of the craniofacial region, as this area is still very new and evolving.

Table 1. Definition of landmarks identified using Dolphin Imaging Software

Anterior Nasal Spine (ANS)	The most anterior point of the anterior nasal spine of the maxilla
Posterior Nasal Spine (PNS)	The most posterior point of the posterior nasal spine of the palatine bones
Menton	A midline point at the most inferior point of the mandibular symphysis
Mental Foramen (Right & Left)	The center of the opening where the inferior alveolar nerve emerges on the facial surface of the mandible
Gonion (Right & Left)	The point along the angle of the mandible at which a perpendicular line drawn from the angle of the mandible passes through the intersection of a line drawn along the inferior border of the mandibular body and another drawn along the posterior border of the mandibular ramus
Condylion (Right & Left)	The most superior point on the mandibular condyle
Maxillary Tuberosity (Right & Left)	The most posterior, lateral, inferior point on the maxilla
Zygomatic Prominence (Right & Left)	The most anterior point on the zygoma in the area of the zygomatico-maxillary suture
Mandibular alveolar midline	The midpoint between the apices of the mandibular central incisors
Maxillary Alveolar Midline	The midpoint between the apices of the maxillary central incisors
Genial Tubercle	The point on the inner surface of the mandible that serves as attachment for the geniohyoid and genioglossus muscles

Table 2. Definition of linear and angular measurements taken using Dolphin Imaging Software

Nasal height (Right & Left)	The linear distance between the most anterior-inferior portion of the nasal passage and the anterior-inferior portion of the nasal bone
Mandibular length, 1 (Right & Left)	The linear distance between points Condylion and Menton
Mandibular length, 2 (Right & Left)	The linear distance between points Condylion and Gonion PLUS the linear distance between points Gonion and Menton (Co-Go + Go-Me)
Ramal height (Right & Left)	The linear distance between points Condylion and Gonion
Mandibular body length (Right & Left)	The linear distance between points Gonion and Menton
Gonial angle (Right & Left)	The angle formed between points Condylion, Gonion, and Menton, with Gonion at the vertex

The output from each set of results was exported to Microsoft Excel (Redmond, WA) and saved using the patient identifier.

Evaluation of Landmarks

The coordinate and linear data from the ten subjects repeated during the study were evaluated for reproducibility with the Bland-Altman test. The coordinate data were evaluated for all three planes and graphed with their confidence intervals. Correlation coefficients were also calculated for each plane.

To determine each landmark's specific envelope of error, the difference between time points for each point on each patient was calculated, and then the absolute value of the difference was averaged with the same point on all ten subjects. The data from the

right and left sides were combined for bilateral points, for example, right condylion and left condylion data were combined to determine overall error of the point. The absolute value (i.e. elimination of positive or negative assignments to values) was used because this study was not designed to study right versus left differences. For example, if the second measurement was more to the right on the x axis, the value would be positive, while a second measurement to the left would be negative. The absolute value of the difference eliminates distortion based on right versus left error. The average error and standard deviation were calculated for the X, Y, and Z axes and linear measurements.

The output data were evaluated to generate an asymmetry index for a given patient. For each bilateral point, the equation $\sqrt{(x_1-x_2)^2+(y_1-y_2)^2+(z_1-z_2)^2}$ was used to find the asymmetry index as proposed by Katsumata,³⁹ where x_1 , y_1 , and z_1 are the coordinates from the right side, and x_2 , y_2 , and z_2 are the coordinates from the left side. The asymmetry index is equivalent to the three-dimensional vector difference from the 0,0,0 orientation point between the right and left sides. For unilateral or midline points, the absolute value of x was used to determine asymmetry, as there is no vertical or sagittal reference from which to determine symmetry. For linear and angular measurements, $\sqrt{(x_1-x_2)^2}$ was used where x_1 is the linear or angular measurement on the right side, while x_2 is the linear or angular measurement on the left side of the head. The mean asymmetry index and standard deviation of each measurement for both the symmetric and asymmetric subjects were calculated and compared with a two-tailed unequal variance Student's t test.

The mean asymmetry index and standard deviation for each point for the symmetric subjects were plotted on a graph with a demarcation for the average value and one and two standard deviations above the mean. This produced a graphical asymmetry index demonstrating the amount of asymmetry in those specified points for our non-asymmetric sample. The asymmetry index from asymmetric subjects was calculated in an identical way, however, the data were not pooled with the symmetric individuals.

RESULTS

Reliability of Orientation Method

The five scans repeated to test reproducibility of orientation were statistically analyzed with the Bland-Altman test for reproducibility. Additionally, a linear regression analysis was performed. The Bland-Altman testing showed an acceptable distribution of points. The linear regression analysis showed an R^2 value of 0.93 for the X axis, 0.99 for the Y axis, 0.99 for the Z axis. The results are displayed in Figures 2-7.

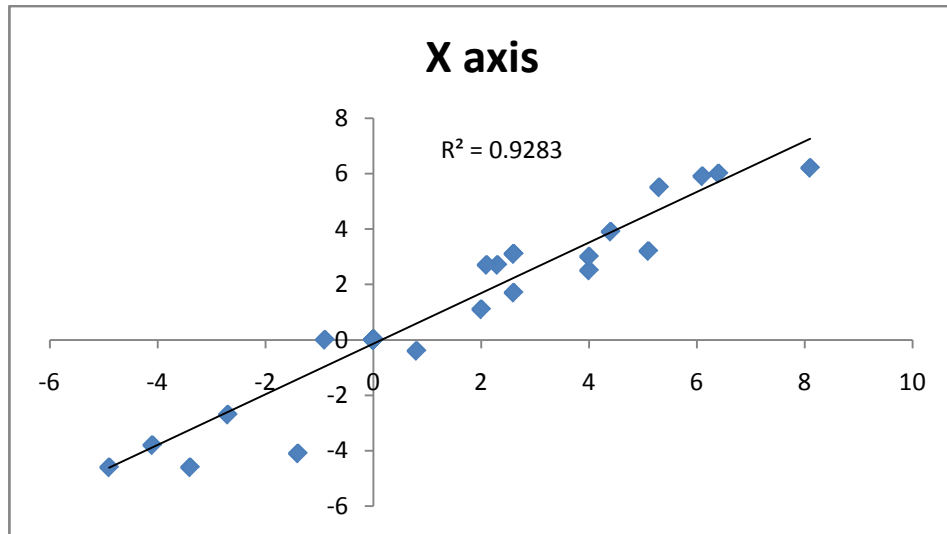


Figure 2. Graphic representation of the linear regression analysis of repeated measures of the X axis from five repeated scans, used to evaluate the orientation method. Time point 1 values (x axis) are plotted against time point 2 values (y axis).

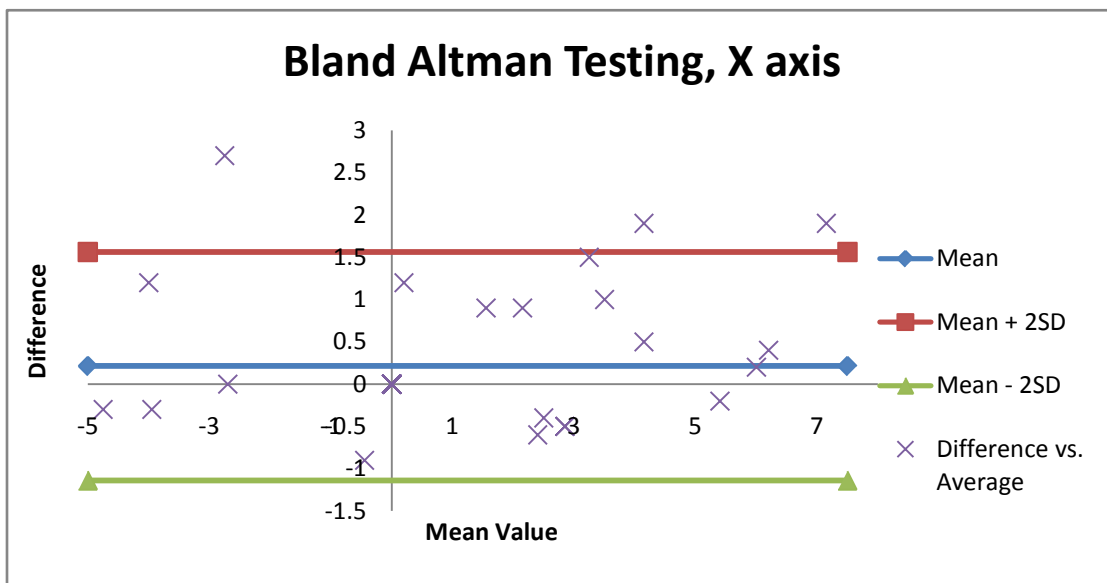


Figure 3. Graphic representation of the Bland-Altman test for the X axis from five repeated scans, used to evaluate the orientation method. The mean values of the two time points (x axis) are plotted against the difference between the two values (y axis).

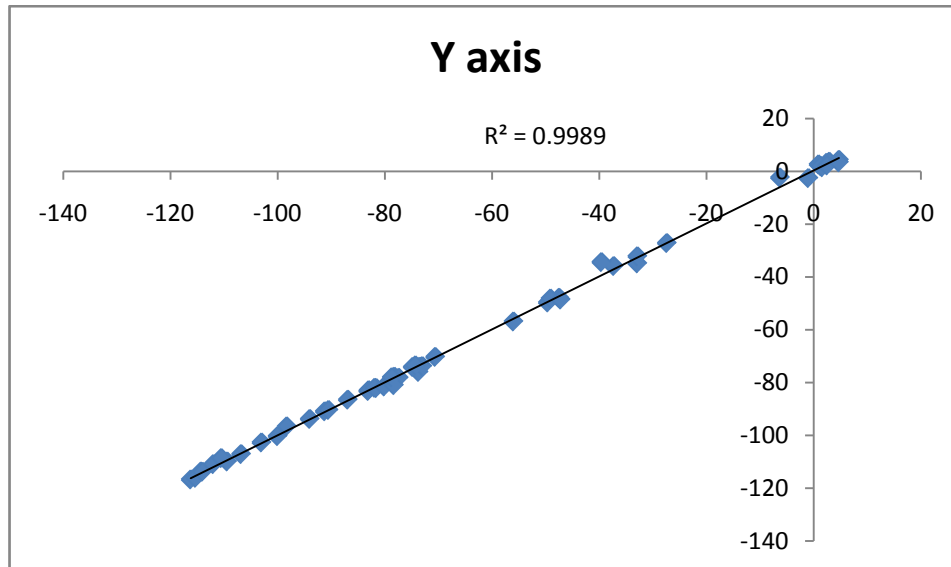


Figure 4. Graphic representation of the linear regression analysis of repeated measures of the Y axis from five repeated scans, used to evaluate the orientation method. Time point 1 values (x axis) are plotted against time point 2 values (y axis).

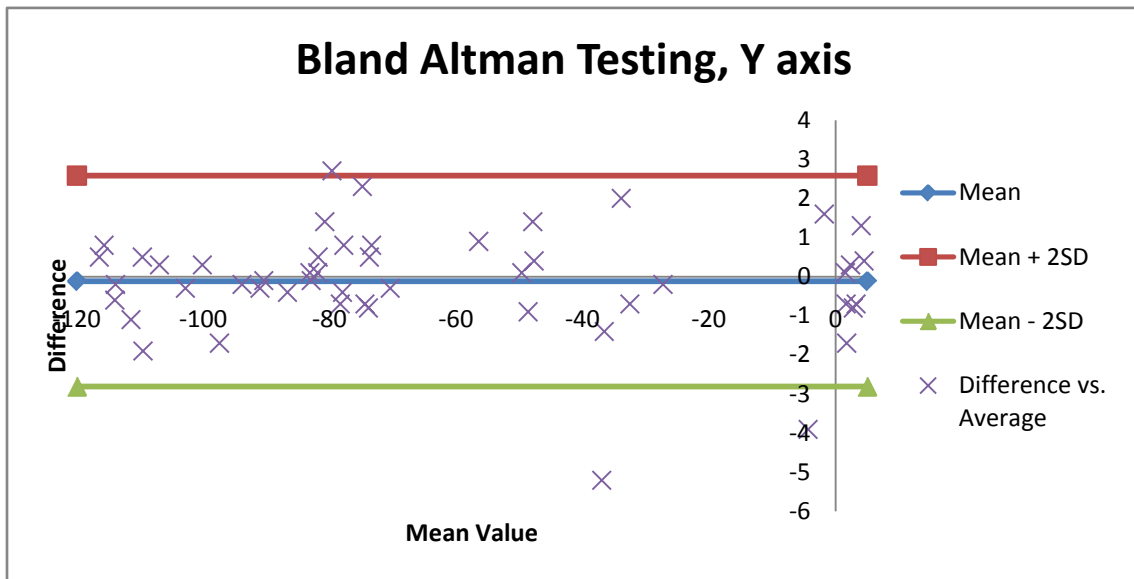


Figure 5. Graphic representation of the Bland-Altman test for the Y axis from five repeated scans, used to evaluate the orientation method. The mean values of the two time points (x axis) are plotted against the difference between the two values (y axis).

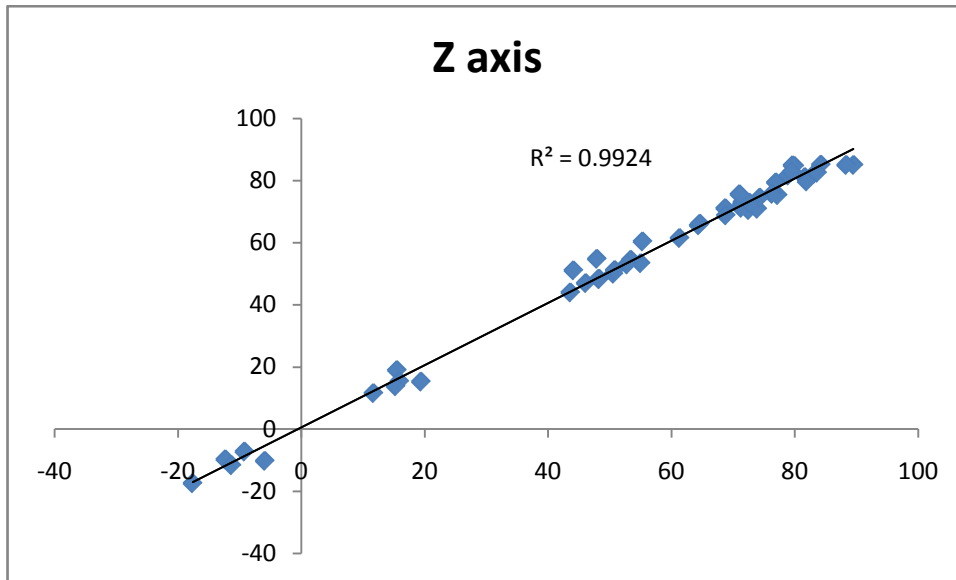


Figure 6. Graphic representation of the linear regression analysis of repeated measures of the Z axis from five repeated scans, used to evaluate the orientation method. Time point 1 values (x axis) are plotted against time point 2 values (y axis).

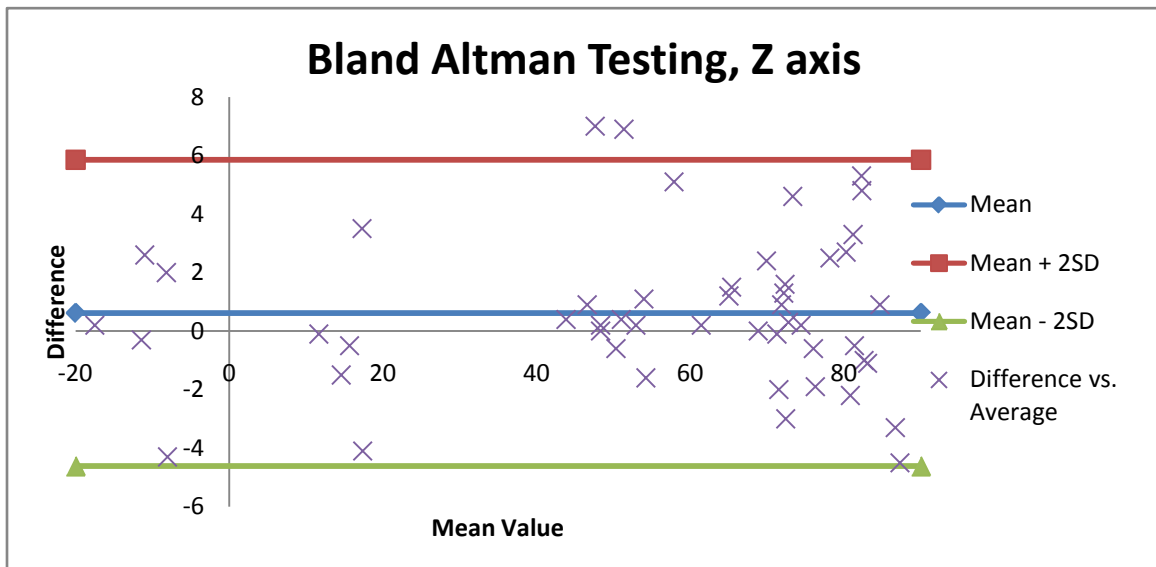


Figure 7. Graphic representation of the Bland-Altman test for the Z axis from five repeated scans, used to evaluate the orientation method. The mean values of the two time points (x axis) are plotted against the difference between the two values (y axis).

The raw data are listed in Table 3 below. The mean difference and standard deviations between the two time points for the landmarks are listed for all three axes. Additionally in Table 4, the three dimensional error was calculated from that data with the equation $\sqrt{(x^2+y^2+z^2)}$. This total three dimensional error, defined as identification error in which orientation was not a factor, was compared to three-dimensional error from Schlicher's work.⁴¹ Identification error was subtracted from total error to find error attributable to the orientation method.

Landmark	Mean X Difference \pm S.D.	Mean Y Difference \pm S.D.	Mean Z Difference \pm S.D.
Sella	0.00 \pm 0.00	1.18 \pm 1.54	1.94 \pm 1.79
Basion	0.00 \pm 0.00	1.90 \pm 1.97	1.88 \pm 1.71
Nasion	0.18 \pm 0.40	1.12 \pm 0.60	1.96 \pm 1.64
R Maxillary Incisor Tip	0.90 \pm 1.10	0.64 \pm 0.48	1.90 \pm 1.64
L Maxillary Incisor Tip	0.92 \pm 0.90	1.20 \pm 1.23	1.74 \pm 2.07
ANS	0.00 \pm 0.00	0.74 \pm 0.50	1.92 \pm 1.56
Menton	0.00 \pm 0.00	0.64 \pm 0.31	2.18 \pm 2.76
Gnathion	0.00 \pm 0.00	0.66 \pm 0.71	2.06 \pm 2.80
L Mandibular Incisor Tip	0.76 \pm 0.46	0.60 \pm 0.23	1.88 \pm 1.88
L Mandibular Incisor Root Apex	0.84 \pm 0.29	0.54 \pm 0.66	2.02 \pm 2.08

Table 3. The mean difference and standard deviation in millimeters between repeated time points for ten landmarks with high inter-rater reliability on five subjects.

Landmark	3D Total Error $\sqrt{(x^2+y^2+z^2)}$	3D Identification Error	Error attributable to orientation method
Sella	2.27	0.41	1.86
Basion	2.67	0.58	2.09
Nasion**	2.26	0.85	1.41
R Maxillary Incisor Tip	2.20	0.53	1.67
L Maxillary Incisor Tip	2.31	0.51	1.80
ANS**	2.06	0.96	1.10
Menton**	2.27	1.44	0.83
Gnathion**	2.16	1.26	0.90
L Mandibular Incisor Tip**	2.11	0.86	1.25
L Mandibular Incisor Root Apex**	2.25	1.18	1.07

Table 4. The mean three-dimensional error in millimeters of ten highly reproducible landmarks on five subjects and the amount of error calculated from landmark identification without error for head orientation. Error attributed to orientation method is calculated by subtracting identification error from total error.

** = measurements where error attributable to orientation method is less than 1.5mm

Reproducibility of Study Landmarks and Measurements

Measurements were taken on separate sessions using the Dicom data sets of ten subjects. The results of these measurements were compared by a Bland-Altman test and a linear regression analysis. The Bland-Altman values showed an acceptable distribution of points. The linear regression analysis showed an R^2 value of 0.99 for the X, Y, and Z axes. These results are shown in Figures 8-15.

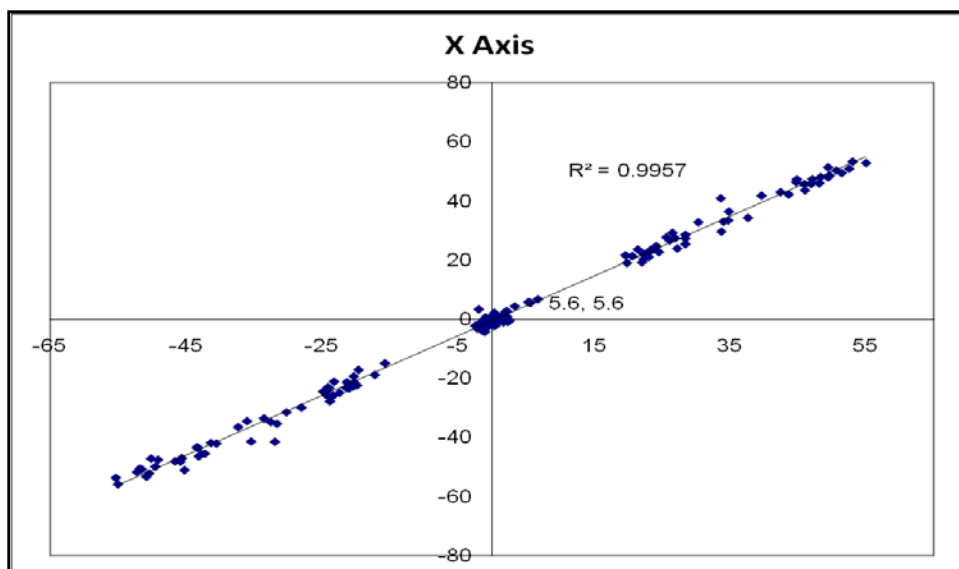


Figure 8. Graphic representation of the linear regression analysis of repeated measures of the X axis, used to evaluate the landmark reproducibility from ten repeated scans. Time point 1 values (x axis) are plotted against time point 2 values (y axis).

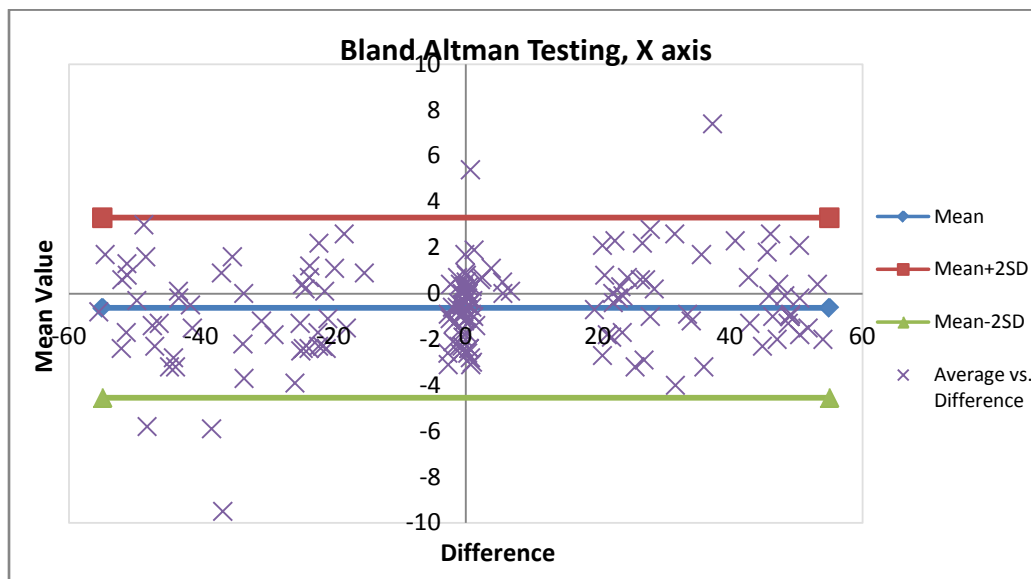


Figure 9. Graphic representation of the Bland-Altman test for the X axis, used to evaluate landmark reproducibility from ten repeated scans. The mean values of the two time points (x axis) are plotted against the difference between the two values (y axis).

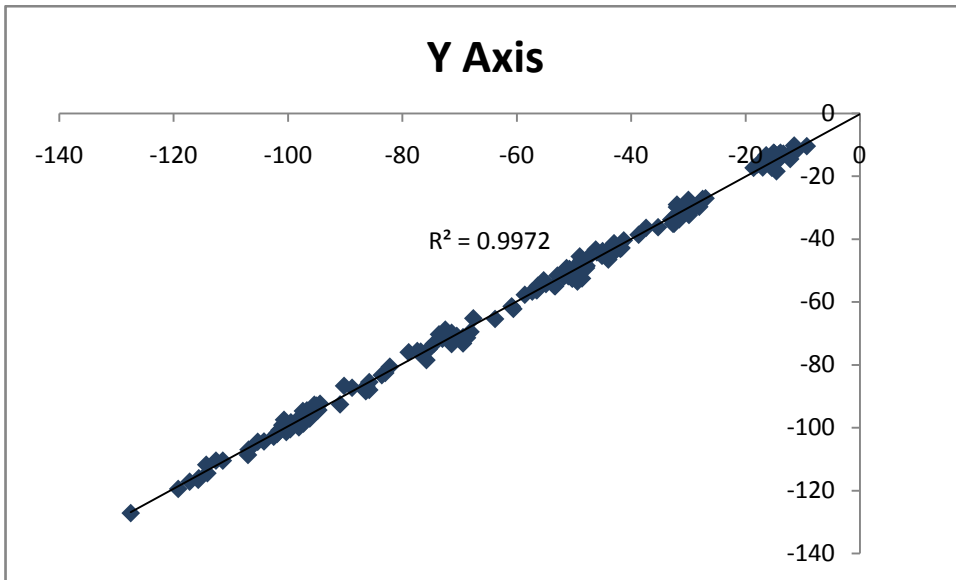


Figure 10. Graphic representation of the linear regression analysis of repeated measures of the Y axis, used to evaluate the landmark reproducibility from ten repeated scans. Time point 1 values (x axis) are plotted against time point 2 values (y axis).

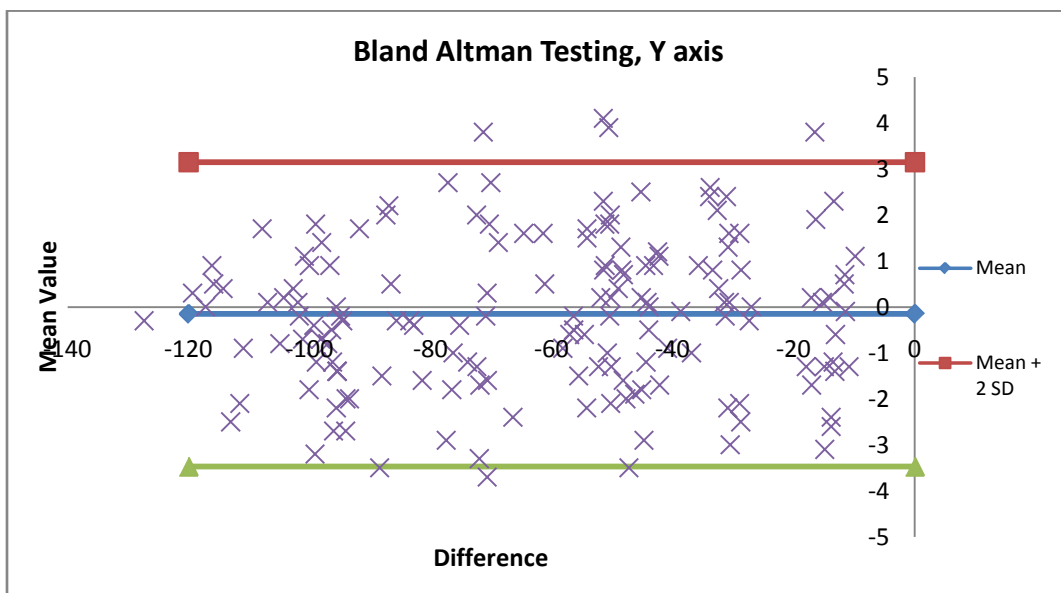


Figure 11. Graphic representation of the Bland-Altman test for the Y axis, used to evaluate landmark reproducibility from ten repeated scans. The mean values of the two time points (x axis) are plotted against the difference between the two values (y axis).

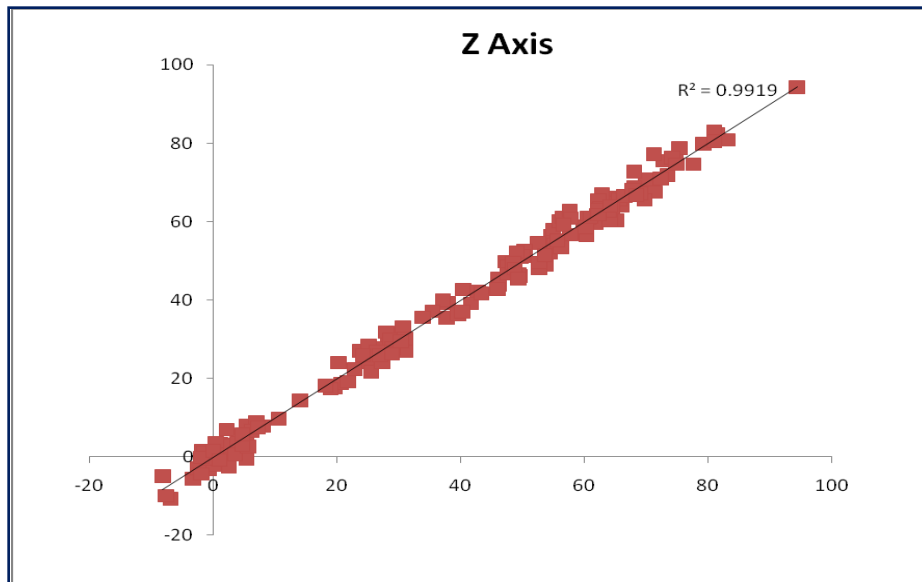


Figure 12. Graphic representation of the linear regression analysis of repeated measures of the Z axis, used to evaluate the landmark reproducibility from ten repeated scans. Time point 1 values (x axis) are plotted against time point 2 values (y axis).

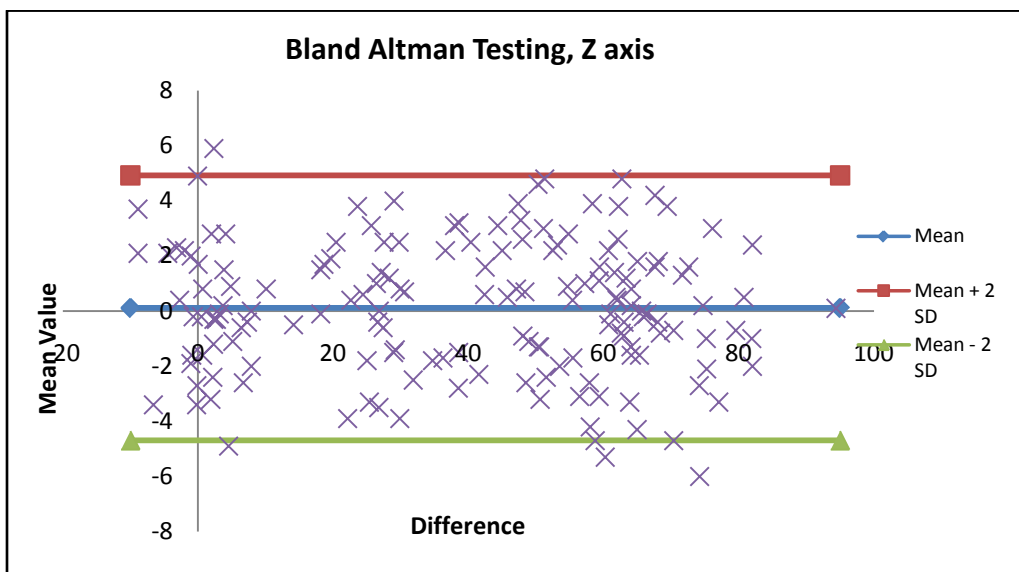


Figure 13. Graphic representation of the Bland-Altman test for the Z axis, used to evaluate landmark reproducibility from ten repeated scans. The mean values of the two time points (x axis) are plotted against the difference between the two values (y axis).

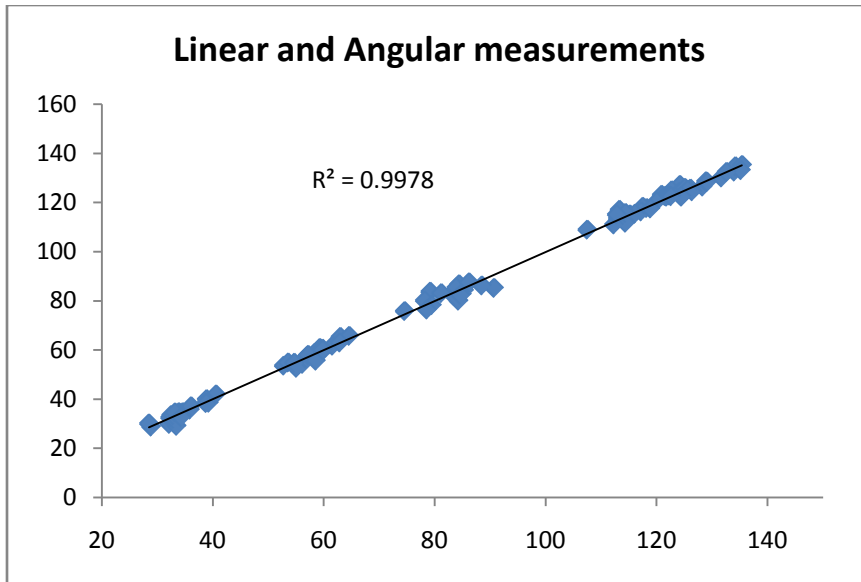


Figure 14. Graphic representation of the linear regression analysis of repeated measures of the linear and angular measurements, used to evaluate the landmark reproducibility from ten repeated scans. Time point 1 values (x axis) are plotted against time point 2 values (y axis).

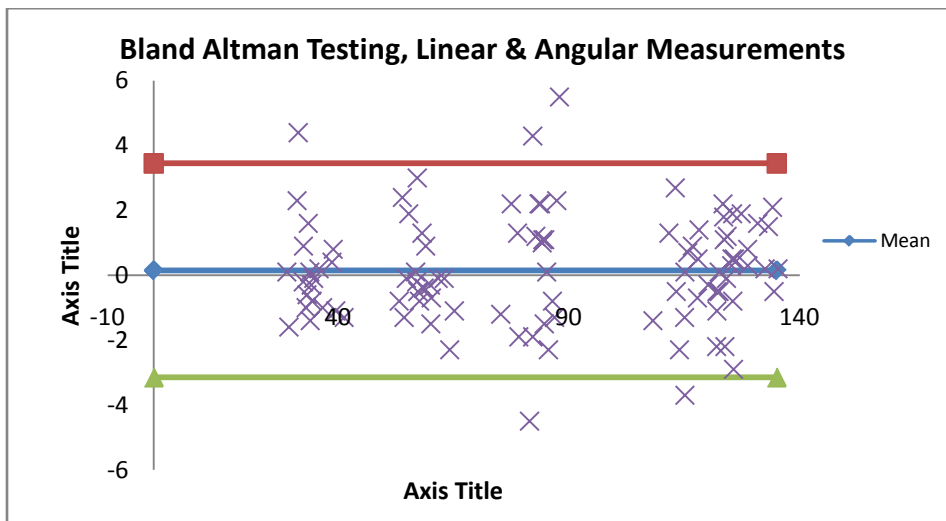


Figure 15. Graphic representation of the Bland-Altman test for the linear and angular measurements, used to evaluate landmark reproducibility from ten repeated scans. The mean values of the two time points (x axis) are plotted against the difference between the two values (y axis).

Regarding specific landmarks and their envelope of error, the means and standard deviations of the average difference between measurements are listed in Tables 5 and 6.

Landmark	X axis	Y axis	Z axis
ANS**	1.09 ± 0.71	1.21 ± 1.21	1.52 ± 1.07
PNS	1.53 ± 1.56	1.00 ± 0.56	1.59 ± 1.06
Menton	0.92 ± 0.87	0.81 ± 0.84	2.34 ± 1.46
Mental Foramen	1.31 ± 0.99	0.92 ± 0.71	2.14 ± 1.33
Gonion	1.25 ± 0.95	1.89 ± 1.08	2.16 ± 1.46
Condylion	1.73 ± 1.17	1.39 ± 1.06	1.43 ± 1.36
Maxillary Tuberosity	1.73 ± 1.06	1.66 ± 1.01	2.14 ± 1.24
Zygomatic Process	2.66 ± 2.45†	1.37 ± 0.98	1.65 ± 1.41
Mandibular Alveolar Midline	1.33 ± 1.09	1.53 ± 1.03	2.90 ± 1.81†
Maxillary Alveolar Midline**	0.82 ± 0.84	0.97 ± 0.55	1.34 ± 0.94
Genial Tubercle	1.34 ± 1.15	1.52 ± 1.01	2.63 ± 1.47†

Table 5. Mean difference and standard deviation of repeated landmark measurements, in millimeters. Data were pooled for bilateral points.

** = all three axes have less than a 1.5mm average variation

† = axis which has a variation of greater than 2.5mm

Landmark Measurement	Difference \pm St. Dev.
Nasal Height**	1.01 \pm 0.96
Mandibular Length (Co-Me)**	1.04 \pm 0.69
Ramus Height**	0.99 \pm 0.82
Mandibular Body Length (Go-Me)	2.00 \pm 1.34
Gonial Angle**	1.31 \pm 1.05

Table 6. Mean difference and standard deviation for linear and angular measurements, in millimeters or degrees. Data were pooled for bilateral points.

** = measurements where the average difference was less than 1.5mm or degrees

Asymmetry Index Values

The mean asymmetry index for each point and linear and angular measurement was calculated and averaged for both groups of subjects. A two-tailed unequal variance Student's t-test was performed to determine significance between the two groups for each measurement (significance $p < 0.05$). The results are listed in Table 7. The average asymmetry indices were found to be statistically significantly different between nine points: Menton, Mental Foramen, Gonion, Condylion, Zygomatic Prominence, Mandibular Alveolar Midline, Genial Tubercle, Mandibular Body (Go-Me), Mandibular Length (Co-Me and Co-Go + Go-Me), and Gonial Angle.

Landmark	Symmetric Subjects, n=32		Asymmetric Subjects, N=18		t-test
	Mean	SD	Mean	SD	
ANS	0.88	0.66	0.71	0.64	0.380
PNS	0.86	0.70	0.83	0.64	0.879
Tuberosity	2.75	1.51	3.29	1.70	0.270
Zygomatic Prominence	2.77	1.26	3.77	2.06	0.075
Maxillary Alveolar Midline	0.88	0.58	1.01	0.66	0.488
Nasal Height	0.74	0.57	1.33	1.54	0.130
Menton	1.15	0.84	3.51	2.21	0.000**
Mental Foramen	2.75	1.07	5.97	3.22	0.001**
Mandibular Alveolar Midline	0.88	0.64	2.79	1.78	0.000**
Genial Tubercle	1.03	0.69	2.63	1.90	0.002**
Gonion	3.49	1.28	5.34	2.92	0.021**
Condylion	2.92	1.19	4.54	2.04	0.005**
Ramus Height (Co-Go)	1.36	1.07	2.13	1.67	0.090
Mandibular Body Length (Go-Me)	1.33	1.07	2.61	2.33	0.039**
Mandibular Length (Co-Go+Go-Me)	1.44	1.13	2.96	2.98	0.049**
Mandibular Length(Co-Me)	1.35	0.79	2.70	2.36	0.030**
Gonial Angle	2.01	1.33	2.77	2.79	0.282

Table 7. Mean and standard deviation of the Asymmetry Index values for both clinically symmetric and asymmetric subjects. ** = $p < 0.05$

The Asymmetry Index for subjects without clinical asymmetry was plotted on a graph, shown below in Figure 16 as a dotted line. The Asymmetry Index plus one standard deviation is plotted as a line between the yellow and green areas. The Asymmetry Index plus two standard deviations is plotted as a line between the yellow

and red areas. On a given patient, a measurement in the green area would be considered “Symmetric,” in the yellow would be considered “Asymmetric,” while measurements in the red area would constitute “Marked Asymmetry.”

The data were plotted in an identical manner for the subjects with clinical asymmetry, as shown in Figure 3. The data for the two groups were not pooled.

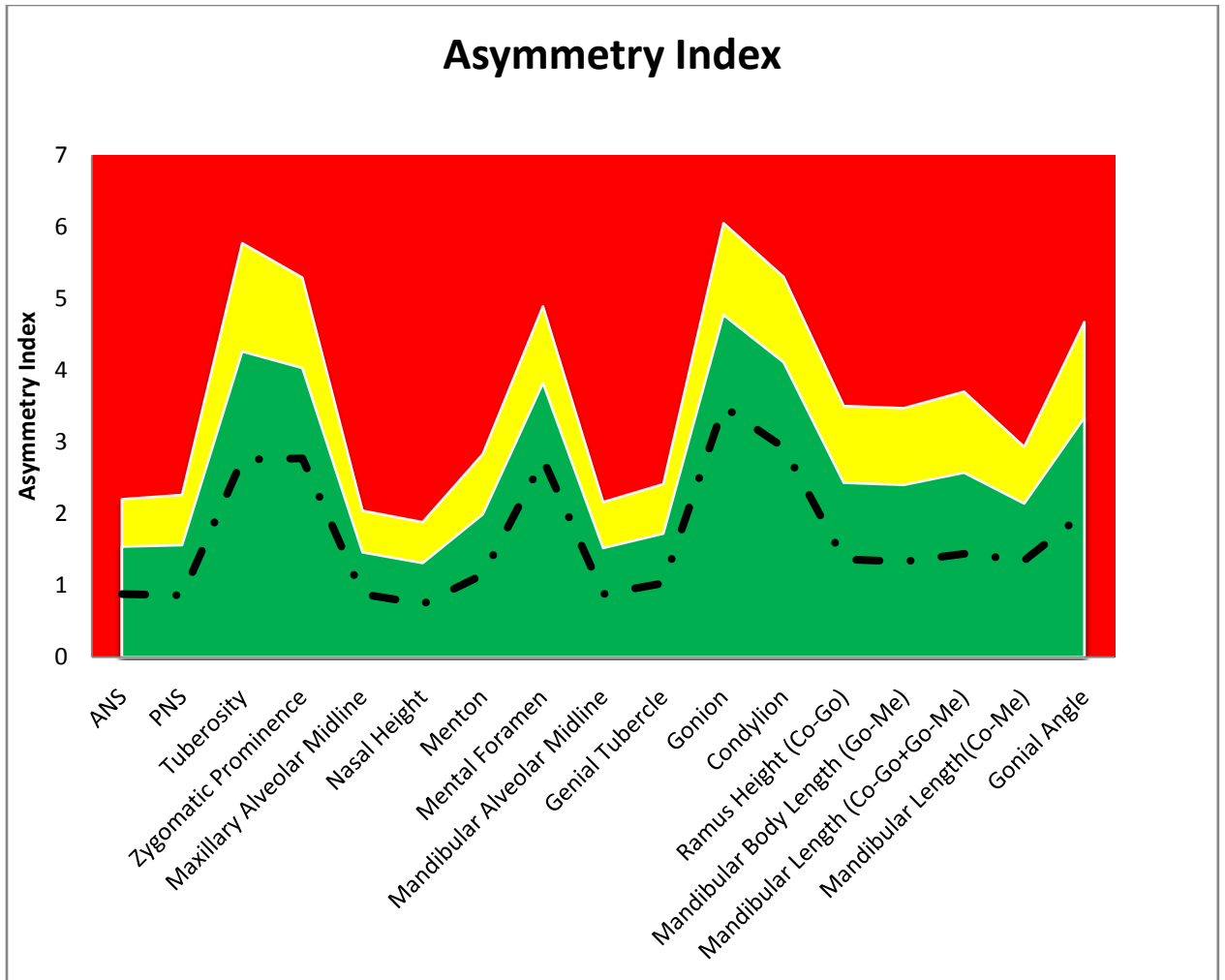


Figure 16. Asymmetry Index for subjects without clinical asymmetry, listed by anatomical region. The dotted line represents average amount of asymmetry for each measurement. The green area represents measurements up to one standard deviation greater than the average asymmetry value, the yellow area represents between one and two standard deviations greater than the mean asymmetry value, and the red area above each point on the graph represents values larger than two standard deviations from the mean.

DISCUSSION

Reproducibility of Head Orientation

The R^2 values of the landmarks are between 0.93-0.99. The Bland-Altman testing also shows an acceptable distribution of points. Only seven of 150 points lie outside the confidence intervals on the graph, which is within the expected statistical error (approximately 3%). There was no systematic error or specific point associated with less reproducibility. However, the absolute differences between the repeated time points are higher than ideal. One must consider the many factors contributing to error associated with identifying a given point. Each of the three reference planes has 1-4 reference points associated with its placement. For example, the X axis plane is through the right and left zygomatico-frontal sutures and parallel to the sella nasion line (four total points). Additionally, each of these reference points has error in three dimensions, which is compounded with the three-dimensional error associated with identification of the specific point being studied. In particular, the Z axis seems to be associated with higher error. From the practical perspective, the bisection of clivus is the most difficult point to identify on the scans, which could explain this increased error. In future work, it would be greatly beneficial to re-define landmarks associated with the Z axis.

A previous study using the same CBCT machine and imaging software had quantified inter-rater reliability of the ten points used for head orientation reproducibility. In this thesis, this error is called “three-dimensional identification error.” The intra-rater

reliability, called “total three-dimensional error,” minus the inter-rater reliability is equal to the error associated with the scan orientation method. Ninety percent of the landmarks showed an orientation error of less than 2mm, while only one point was greater than 2mm (Basion = 2.09mm). This level of error was considered acceptable, though the goal to continuously evaluate ways to reduce error in methods is always present. One must also remember that this head orientation error will be added to the identification error for every point, making the analysis more complex and seemingly more flawed. Reducing head orientation error and increasing reproducibility *must* be a goal of future work in this area.

Reproducibility of Landmark Identification

The R^2 values for reproducibility of study landmarks were very high, >0.99 for all three dimensions as well as linear and angular measurements. The Bland-Altman testing showed 14 errors out of 480 repeated points that were outside the two standard deviation confidence intervals. This is less than 3% and within acceptable statistical variance. There were 4 outliers in the Y axis and 5 errors in the X- and Z- axis and linear measurements. One subject had 7 of these errors on his scan alone. The zygomatic process, condylion, and gonion each had three errors in reproducibility, reflecting the difficulty in accurately reproducing these points.

Looking at the absolute difference in reproducibility, only two landmarks (ANS and maxillary alveolar midline) had error in all three dimensions of less than 1.5-mm.

However, only three points (zygomatic process in the X axis, mandibular midline in the Z axis and genial tubercle Z axis) had error in any dimension greater than 2.5-mm. Eighty percent of the linear and angular measurements were less than 1.5mm of three-dimensional error, while all points were less than 2.0mm. Reflecting what was seen in the evaluation of head position, the Z axis appears to have the greatest error associated with it. The recommendation, again, would be to evaluate a different reference point for the Z axis.

The three dimensional error of individual points, which is representative of total error, is unacceptably high. However, this error includes the three dimensional error associated with head orientation, which was also high. Interestingly, all but one linear measurement had reproducibility error less than 1.5mm. This indicates that there is some noise around the orientation method that may be ignored if one uses linear measurements as the basis for the analysis. All aspects of error must be investigated more fully in an attempt to reduce the error of the method.

Asymmetry in Symmetric Subjects

The most symmetric midline point in the symmetric subjects was the maxillary alveolar midline nasal height ($0.74\text{mm} \pm 0.57\text{mm}$ from the midsagittal plane), the most symmetric bilateral point was the mental foramen ($2.75\text{mm} \pm 1.07\text{mm}$ difference between right and left), while the most symmetric linear measurement was nasal height ($0.74\text{mm} \pm 0.57\text{mm}$ difference between right and left). The least symmetric midline

point was menton ($1.15\text{mm} \pm 0.84\text{mm}$), the least symmetric bilateral point was gonion ($3.49\text{mm} \pm 1.28\text{mm}$), and least symmetric measurement was gonial angle ($2.01^\circ \pm 1.33^\circ$).

These quantified data are useful as a baseline for future and comparative work. The data showed a high amount of error in the symmetric subjects, but the subject pool was quite varied. Despite a lack of clinical asymmetry, they varied with regard to age, sex, and malocclusion and their underlying skeletal patterns might be quite varied. In future work, additional subjects should be added to test these data. With a large enough sample size, the symmetric subjects could be divided by age, sex, malocclusion, and/or race to further refine the average data.

Asymmetry in Asymmetric Subjects

The most symmetric midline point in the asymmetric individuals was ANS ($0.71\text{mm} \pm 0.64\text{mm}$), the most symmetric bilateral point was the maxillary tuberosity ($3.29\text{mm} \pm 1.70\text{mm}$), and the most symmetric linear measurement was nasal height ($1.33\text{mm} \pm 1.54\text{mm}$). The least symmetric midline point was menton ($3.51\text{mm} \pm 2.21\text{mm}$), the least symmetric bilateral point was mental foramen ($5.97\text{mm} \pm 3.22\text{mm}$), and the least symmetric measurement was mandibular length, condylion-gonion + gonion-menton ($2.96\text{mm} \pm 2.98\text{mm}$).

One limitation of this study is the heterogeneity of the asymmetric subjects. There was no restriction on the amount of clinical asymmetry needed to be classified

“clinically asymmetric.” Therefore, some of the individuals had marked asymmetry, while others had relatively subtle asymmetry. In a sample of 19 subjects, this results in large standard deviations which may affect the interpretation of the results.

The points that were statistically different between the groups of symmetric and asymmetric subjects were menton, mental foramen, mandibular alveolar midline, genial tubercle, gonion, condylion, mandibular body length (gonion to menton), and mandibular length (measured as condylion to menton or condylion to gonion plus gonion to menton). Several of the points studied were in the maxilla, but the inclusion criteria was asymmetry in the mandible, so it is not surprising that no statistical significance was found between maxillary measurements in the two groups. However, it is encouraging that this analysis did detect statistical differences between nearly all points in the mandible.

Clinical Application of Findings

Any measurements that lie within the green area on the map are within one standard deviation of the mean values from the symmetric group, which equals 84% of the sample. Measurements in the yellow area are within one and two standard deviations from the mean (84-97%), while any measurements in the red area represent greater than two standard deviations from the mean, or the 3% most asymmetric values.

An individual's measurements can be superimposed on the graph of the average asymmetry values. Since the measurements are arranged anatomically, this superimposed graph can visually help the clinician determine where exactly the asymmetry is located.

Examples

Listed below are two examples of how the asymmetry index can be applied to individuals, one with mild and one with more marked asymmetry.

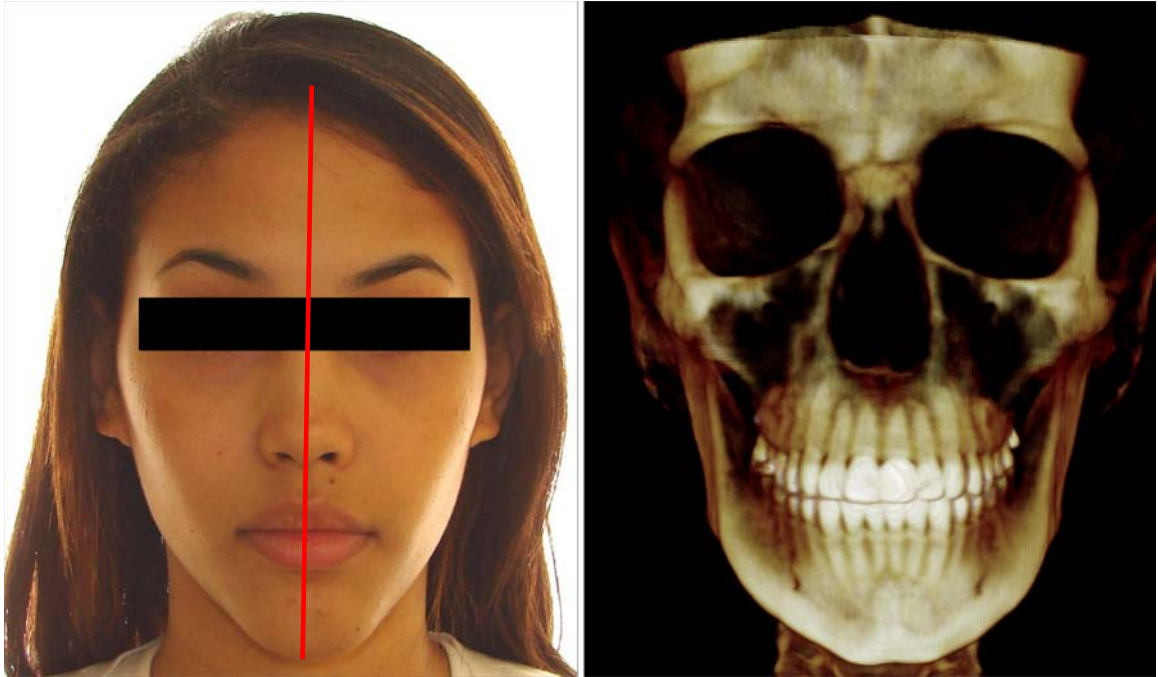


Figure 17. Subject CLMP39. This subject has a mild asymmetry with a chin point deviation to the left. Her clinical photograph and frontal view 3D-CBCT volumetric rendering are shown. Her occlusion appears to be symmetric, with only a mild cant and deviation of the lower incisors. The red line indicates the mid-sagittal plane.

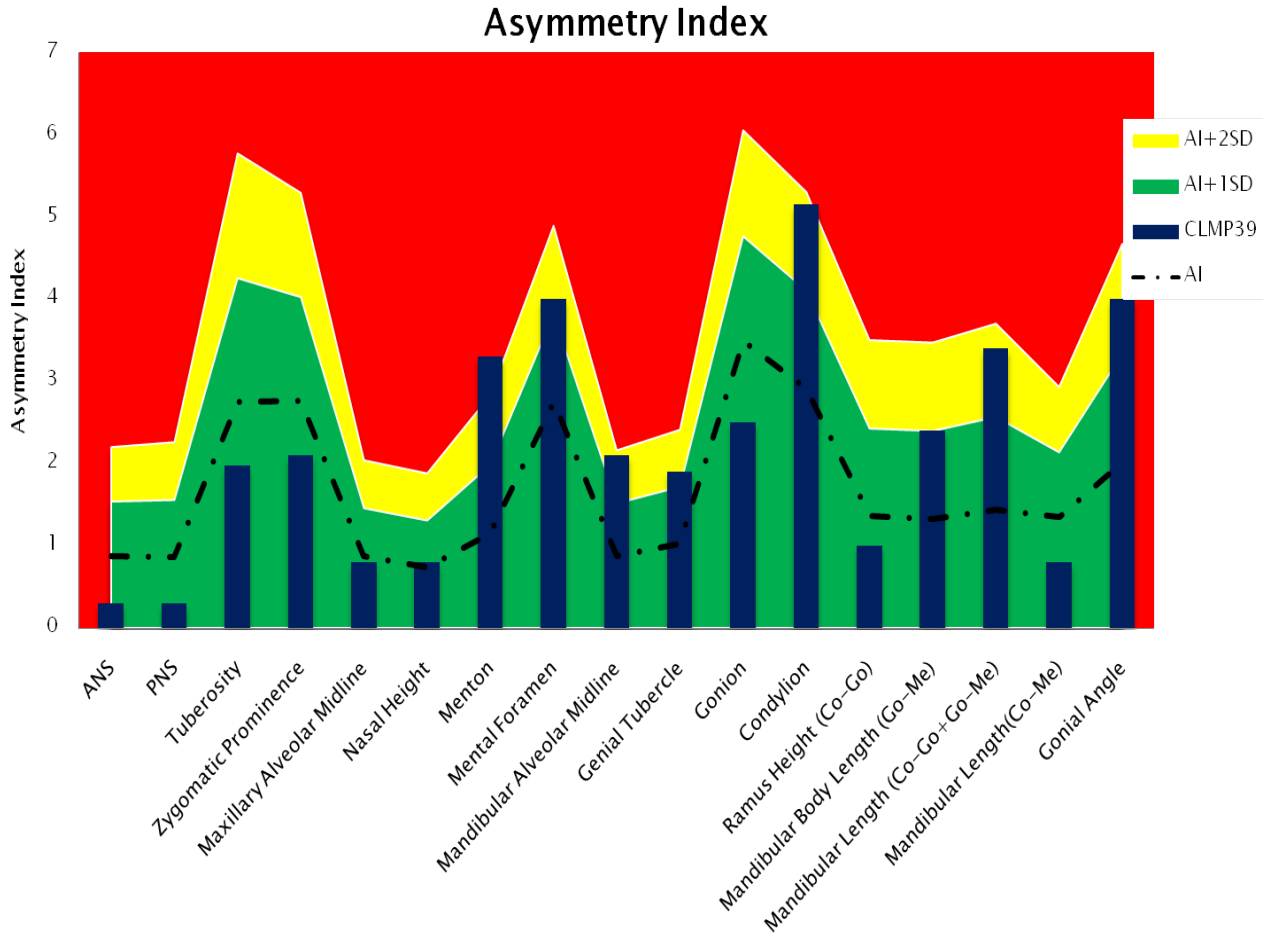


Figure 18. The individual overlay of subject CLMP 39. Mental foramen, condylion, mandibular length (condylion-gonion + gonion-menton), and gonial angle are all between one and two standard deviations larger than the mean. Only one point, menton, is in the red area of the graph. Interpretation of these data indicates that the subject's mild asymmetry could be corrected with a genioplasty, if she would wish.

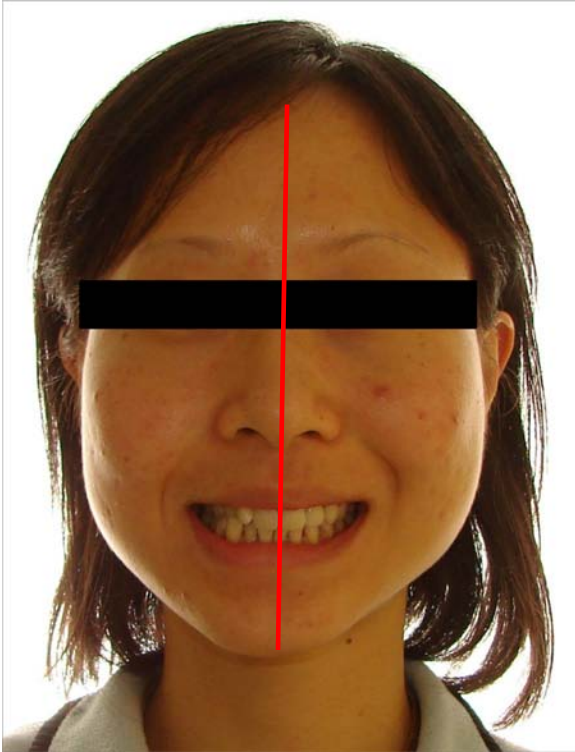


Figure 19. Subject CLMP18. This subject has a marked asymmetry with a chin point deviation to the right. Her clinical photograph and frontal view 3D-CBCT volumetric rendering are shown. Her malocclusion reflects her asymmetry, with a crossbite and midline deviation to the affected side.

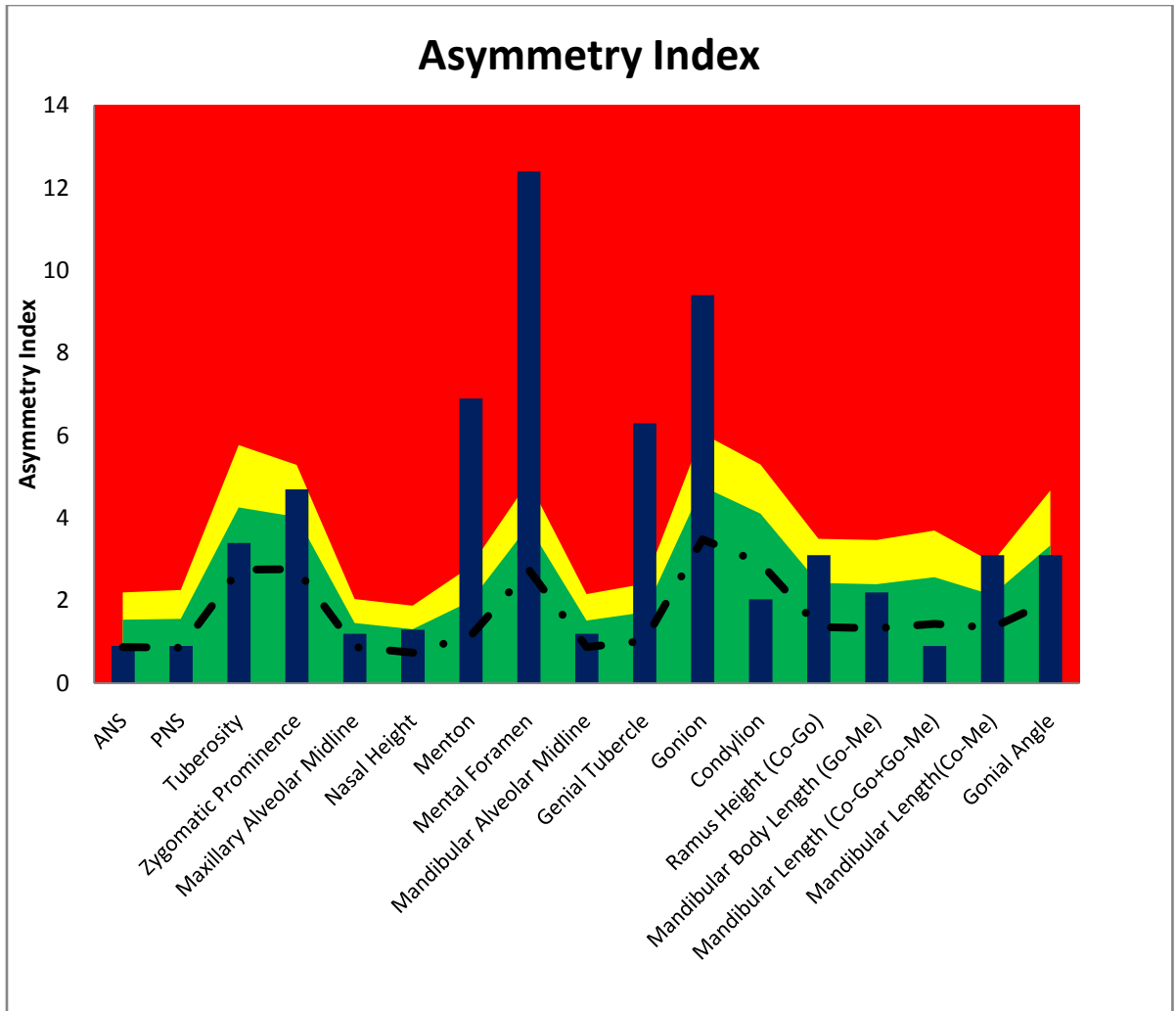


Figure 20. The individual overlay of subject CLMP18. Several points, menton, mental foramen, genial tubercle, and gonion, are in the red area of the graph. The zygomatic processes, ramus height, and mandibular length (condylion-menton) are all between one and two standard deviations larger than the mean. Interpretation of these data indicates that the subject's asymmetry best could be corrected with a mandibular surgery, in which the distal segment is rotated to correct the asymmetry and the proximal segments are held in their current position.

CONCLUSION

This work represents a starting point in the field of asymmetry analysis with cone-beam computed tomography. One of the major concerns in studies concerning landmark analysis is error, and this study has identified specific factors that contribute high amounts of error. Reproducibility of individual points is challenging, mostly due to the complexity of defining the three orientation planes and locating the three-dimensional points. However, reproducibility of linear measurements and angles has a much lower associated error. Building on that observation, the main suggestion for future work would be to base the analysis more heavily on linear and angular measurements and to re-evaluate the landmark used to orient the Z-axis. The anterior wall of sella may be a suitable substitute for the current point, the bisection of clivus.

The sample studied may have limited the quality of the results. Only 33 subjects fit the strict definition of symmetry in this study. These subjects varied widely with regard to malocclusions, age, sex, and race. Additionally, only 18 individuals fit the asymmetry criteria and their asymmetries were quite varied. Another aspect of concern regarding the sample is that the data were collected retrospectively. Ideally, the individuals would have been chosen in a prospective manner. As the UCSF Orthodontic Clinic continues to collect records on CBCT, a larger sample will be accumulated and future studies could be planned to more carefully examine larger groups of both symmetric and asymmetric individuals and subgroups of each. Even with the limitations

of this study sample, statistical differences were found between mandibular measurements in the symmetric and asymmetric groups.

With data from this study, a graphic representation of an individual's asymmetry can easily be compared to the average values and standard deviations of a group of clinically symmetric subjects. The Asymmetry Index can help with localization of the origin of the asymmetry, assisting the clinician in treatment planning. Additionally, this method can be used to undertake longitudinal studies of individuals with asymmetry to better understand their growth, progression of asymmetry, and treatment effects. While this method has some areas that need improvement, particularly related to error associated with landmark identification, this project offers a strong start into the field of CBCT analysis of asymmetry.

No soft tissue points were evaluated in this study. Soft tissue camouflage can mask the severity of the underlying skeletal asymmetry and should be considered when evaluating subjects with skeletal or dental asymmetry. Future work could evaluate soft tissue points and the correlation to skeletal asymmetry, as well as the soft tissue change with skeletal correction. Careful definition of points and identification error studies are needed. The points will undoubtedly be difficult to locate precisely and reproducibly, due to the novelty of the points and the curved surfaces of the soft tissue. Definitions such as "most anterior" or "most lateral" will be useful, especially with a defined head orientation method to help minimize the error.

The future of this approach will be in applying this method to more extreme cases of asymmetry such as hemifacial microsomia (HFM) and cleft lip and/or palate (CL/P). Individuals affected with type III HFM lack traditional craniofacial structures, such as condyles. The definitions used in this study were designed so that they could be used to study these subjects, however, identification error studies will be needed once a sufficient collection of CBCT scans on these types of subjects is available. Using CBCT to follow growth and the effect of treatment is a practical and exciting application of this work for the future. In this study, subjects were not selected for the presence of maxillary or vertical asymmetry, however, that is clearly another potential application of this method. Individuals with CL/P have maxillary skeletal and soft tissue asymmetries, while subjects with vertical canting of the maxilla also present a challenging diagnostic problem. Development of an asymmetry index to encompass vertical and maxillary asymmetries should be initiated and combined with the horizontal asymmetry index developed in this study. In depth studies to understand the growth, development, treatment planning and treatment outcomes of individuals with craniofacial anomalies could then be initiated and would be the ultimate goal of this work. This project identifies some limitations of the current methodology and provides a basis for this exciting future work.

References

1. Lundstrom A. Asymmetries of the Dental Arches, Jaws, and Skull, and their Etiological Significance. *American Journal of Orthodontics* 1961;47:26.
2. Zaidel DW, Deblieck C. Attractiveness of natural faces compared to computer constructed perfectly symmetrical faces. *Int J Neurosci* 2007;117:423-431.
3. Ferrario VF, Sforza C, Miani A, Jr., Serrao G. A three-dimensional evaluation of human facial asymmetry. *J Anat* 1995;186 (Pt 1):103-110.
4. Ferrario VF, Sforza C, Poggio CE, Tartaglia G. Distance from symmetry: a three-dimensional evaluation of facial asymmetry. *J Oral Maxillofac Surg* 1994;52:1126-1132.
5. Cheney EA. Dentofacial asymmetries and their clinical significance. *American Journal of Orthodontics* 1961;47:814-829.
6. Vig PS, Hewitt AB. Asymmetry of the human facial skeleton. *Angle Orthod* 1975;45:125-129.
7. Shah SM, Joshi MR. An assessment of asymmetry in the normal craniofacial complex. *Angle Orthod* 1978;48:141-148.
8. Trpkova B, Prasad NG, Lam EW, Raboud D, Glover KE, Major PW. Assessment of facial asymmetries from posteroanterior cephalograms: validity of reference lines. *Am J Orthod Dentofacial Orthop* 2003;123:512-520.
9. Mulick JF. An Investigation of Craniofacial Asymmetry Using the Serial Twin-Study Method. *Am J Orthod* 1965;51:112-129.
10. Chebib FS, Chamma AM. Indices of craniofacial asymmetry. *Angle Orthod* 1981;51:214-226.

11. Ricketts RM. Perspectives in the clinical application of cephalometrics. The first fifty years. *Angle Orthod* 1981;51:115-150.
12. Grayson B, Cutting C, Bookstein FL, Kim H, McCarthy JG. The three-dimensional cephalogram: Theory, technique, and clinical application. *American Journal of Orthodontics and Dentofacial Orthopedics* 1988;94:11.
13. Forsberg CT, Burstone CJ, Hanley KJ. Diagnosis and treatment planning of skeletal asymmetry with the submental-vertical radiograph. *Am J Orthod* 1984;85:224-237.
14. Kaban LB, Mulliken JB, Murray JE. Three-dimensional approach to analysis and treatment of hemifacial microsomia. *Cleft Palate J* 1981;18:90-99.
15. Letzer GM, Kronman JH. A Posteroanterior Cephalometric Evaluation of Craniofacial Asymmetry. *American Journal of Orthodontics* 1967;37:7.
16. Good S, Edler R, Wertheim D, Greenhill D. A computerized photographic assessment of the relationship between skeletal discrepancy and mandibular outline asymmetry. *Eur J Orthod* 2006;28:97-102.
17. Haraguchi S, Iguchi Y, Takada K. Asymmetry of the face in orthodontic patients. *Angle Orthod* 2008;78:421-426.
18. Azevedo AR, Janson G, Henriques JF, Freitas MR. Evaluation of asymmetries between subjects with Class II subdivision and apparent facial asymmetry and those with normal occlusion. *Am J Orthod Dentofacial Orthop* 2006;129:376-383.
19. Janson GR, Metaxas A, Woodside DG, de Freitas MR, Pinzan A. Three-dimensional evaluation of skeletal and dental asymmetries in Class II subdivision malocclusions. *Am J Orthod Dentofacial Orthop* 2001;119:406-418.

20. Haraguchi S, Takada K, Yasuda Y. Facial asymmetry in subjects with skeletal Class III deformity. *Angle Orthod* 2002;72:28-35.
21. Laspos CP, Kyrkanides S, Tallents RH, Moss ME, Subtelny JD. Mandibular and maxillary asymmetry in individuals with unilateral cleft lip and palate. *Cleft Palate Craniofac J* 1997;34:232-239.
22. Baumrind S, Frantz RC. The reliability of head film measurements. 1. Landmark identification. *Am J Orthod* 1971;60:111-127.
23. Savara BS, Tracy WE, Miller PA. Analysis of errors in cephalometric measurements of three-dimensional distances on the mandible. *Arch Oral Biol* 1966;11:209-217.
24. Major PW, Johnson DE, Hesse KL, Glover KE. Landmark identification error in posterior anterior cephalometrics. *Angle Orthod* 1994;64:447-454.
25. Major PW, Johnson DE, Hesse KL, Glover KE. Effect of head orientation on posterior anterior cephalometric landmark identification. *Angle Orthod* 1996;66:51-60.
26. El-Mangoury NH, Shaheen SI, Mostafa YA. Landmark identification in computerized posteroanterior cephalometrics. *Am J Orthod Dentofacial Orthop* 1987;91:57-61.
27. Ghafari J, Cater PE, Shofer FS. Effect of film-object distance on posteroanterior cephalometric measurements: suggestions for standardized cephalometric methods. *Am J Orthod Dentofacial Orthop* 1995;108:30-37.
28. Kwon TG, Lee KH, Park HS, Ryoo HM, Kim HJ, Lee SH. Relationship between the masticatory muscles and mandibular skeleton in mandibular prognathism with and without asymmetry. *J Oral Maxillofac Surg* 2007;65:1538-1543.

29. Kwon TG, Park HS, Ryoo HM, Lee SH. A comparison of craniofacial morphology in patients with and without facial asymmetry--a three-dimensional analysis with computed tomography. *Int J Oral Maxillofac Surg* 2006;35:43-48.
30. Maki K, Miller AJ, Okano T, Hatcher D, Yamaguchi T, Kobayashi H et al. Cortical bone mineral density in asymmetrical mandibles: a three-dimensional quantitative computed tomography study. *Eur J Orthod* 2001;23:217-232.
31. Hounsfield GN. Computerized transverse axial scanning (tomography). 1. Description of system. *Br J Radiol* 1973;46:1016-1022.
32. Waitzman AA, Posnick JC, Armstrong DC, Pron GE. Craniofacial skeletal measurements based on computed tomography: Part I. Accuracy and reproducibility. *Cleft Palate Craniofac J* 1992;29:112-117.
33. Ludlow JB, Davies-Ludlow LE, Brooks SL, Howerton WB. Dosimetry of 3 CBCT devices for oral and maxillofacial radiology: CB Mercuray, NewTom 3G and i-CAT. *Dentomaxillofac Radiol* 2006;35:219-226.
34. Vannier MW. Craniofacial computed tomography scanning: technology, applications and future trends. *Orthod Craniofac Res* 2003;6 Suppl 1:23-30; discussion 179-182.
35. Greiner M, Greiner A, Hirschfelder U. Variance of landmarks in digital evaluations: comparison between CT-based and conventional digital lateral cephalometric radiographs. *J Orofac Orthop* 2007;68:290-298.
36. Kragsskov J, Bosch C, Gyldensted C, Sindet-Pedersen S. Comparison of the reliability of craniofacial anatomic landmarks based on cephalometric radiographs and three-dimensional CT scans. *Cleft Palate Craniofac J* 1997;34:111-116.

37. Stratemann SA, Huang JC, Maki K, Miller AJ, Hatcher DC. Comparison of cone beam computed tomography imaging with physical measures. *Dentomaxillofac Radiol* 2008;37:80-93.
38. Baek SH, Cho IS, Chang YI, Kim MJ. Skeletodental factors affecting chin point deviation in female patients with class III malocclusion and facial asymmetry: a three-dimensional analysis using computed tomography. *Oral Surg Oral Med Oral Pathol Oral Radiol Endod* 2007;104:628-639.
39. Katsumata A, Fujishita M, Maeda M, Ariji Y, Ariji E, Langlais RP. 3D-CT evaluation of facial symmetry. *Oral Surgery, Oral Medicine, Oral Pathology, Oral Radiology, and Endodontology* 2005;99:9.
40. Maeda M, Katsumata A, Ariji Y, Muramatsu A, Yoshida K, Goto S et al. 3D-CT evaluation of facial asymmetry in patients with maxillofacial deformities. *Oral Surg Oral Med Oral Pathol Oral Radiol Endod* 2006;102:382-390.
41. Schlicher J. Consistency and Precision of Three Dimensional Landmark Identification Unpublished Thesis; 2008.

PUBLISHING AGREEMENT

It is the policy of the University to encourage the distribution of all theses, dissertations, and manuscripts. Copies of all UCSF theses, dissertations, and manuscripts will be routed to the library via the Graduate Division. The library will make all theses, dissertations, and manuscripts accessible to the public and will preserve these to the best of their abilities, in perpetuity.

I hereby grant permission to the Graduate Division of the University of California, San Francisco to release copies of my thesis, dissertation, or manuscript to the Campus Library to provide access and preservation, in whole or in part, in perpetuity.

Carol Jant sup *5/22/09*

Author Signature Date